c1

A THEORY FOR WIND TUNNEL WALL CORRECTIONS.

BY

CHRISTOPHER D. WILLIAMS

B.A.Sc., University of British Columbia, 1967.

A THESIS SUBMITTED IN PARTIAL FULFILMENT OF
THE REQUIREMENTS FOR THE DEGREE OF
MASTER OF APPLIED SCIENCE

in the Department
of
Mechanical Engineering

We accept this thesis as conforming to the
required standard.

THE UNIVERSITY OF BRITISH COLUMBIA

APRIL 1973

In presenting this thesis in partial fulfilment of the requirements for an advanced degree at the University of British Columbia, I agree that the Library shall make it freely available for reference and study. I further agree that permission for extensive copying of this thesis for scholarly purposes may be granted by the Head of my Department or by his representatives. It is understood that copying or publication of this thesis for financial gain shall not be allowed without my written permission.

Department of Mechanical Engineering

The University of British Columbia
Vancouver 8, Canada

Date April 16, 1973

Abstract

Wall correction theories for two-dimensional airfoils in wind tunnels with partly open walls are examined. Conventional wall correction theories are linearized theories, valid only for small thin models of slight camber at low angles of attack. Such theories are shown to be useless for the prediction of the required wall corrections for large models, models at high angles of attack, or models developing high lift.

An exact numerical theory is presented in which it is not necessary to make these assumptions. The airfoil and any solid wall sections are represented by surface source and vortex singularities as in the method of A.M.O.Smith. Aerodynamic lift is determined by numerical integration of the calculated pressure distributions around the airfoil contour. The theory indicates that certain wall configurations will require small or negligible wall corrections for tests on lifting airfoils.

_____

Supervisor

TABLE OF CONTENTS

LIST OF FIGURES AND TABLES

ACKNOWLEDGEMENTS

The author would like to thank Dr. G. V. Parkinson for his advice and guidance in the course of this research.

The computing facilities of the Computing Center of the University of British Columbia were used to do the calculations contained herein.

This research was supported by the University of British Columbia and the Defence Research Board of Canada.

I Introduction

The problem of determining the effect of the walls of a wind tunnel on a model under test is an old one, which has occupied researchers for more than forty years. The problem is extremely complex since the effect of the tunnel walls is to alter the flow conditions (speed and direction) near the model from those that would exist in a corresponding test in free air. At a given point in the flow field these effects are functions of model size and shape. Any measured quantities, such as flow speed or aerodynamic forces and moments, must be corrected for these wall effects. Ideally such corrections could be applied directly to these measured quantities to predict their values as they would be measured in a free-air test environment.

II Conventional Theories for Wall Corrections

Glauert(3), Goldstein(4), and Allen and Vincenti(1) used singularity image techniques to model the airfoil-wall interactions. The lift-producing characteristics of the airfoil, the airfoil thickness, and the airfoil wake are associated with distributions of vortices, doublets, and sources respectively. For each type of singularity, a suitable system of "images" is found in the tunnel walls, to satisfy the required flow conditions at the walls; for example, a solid wall boundary requires zero flow normal to the boundary, while an open jet boundary requires a constant pressure along the boundary. It is very useful if the induced effect of each system of images at the airfoil can be assumed to be additive; that is, these individual effects can be superimposed. In terms of the corresponding field equations, this requires a linearized theory, valid only for small wall effects, that is, for small, thin, slightly cambered airfoils at low angles of attack.

Woods(12) uses conformal mappings to transform the airfoil plus walls into a geometrically simple boundary value problem for which a solution is known; that is, a function of a complex variable whose real and/or imaginary parts are prescribed on this boundary. Woods' technique results in integral equations for the mapping function; usually numerical techniques are required for their solution.

Either approach can be formulated in terms of the disturbance flow velocity potential ϕ, which for incompressible flow satisfies Laplace's equation, which is linear.

For a solid boundary which is parallel to the undisturbed flow at upstream infinity there is zero flow normal to the boundary; hence $\left.\frac{\partial \phi}{\partial n}\right|$ is zero there.

For an open jet the linearized condition of constant pressure at the jet boundary can be expressed via Bernoulli's equation as requiring zero streamwise disturbance velocity; hence $\left.\frac{\partial \phi}{\partial x}\right|$ is zero there.

For slotted or perforated walls where an "equivalent homogeneous boundary condition" can be stipulated, (Baldwin et al(2)), a linear combination of the boundary conditions for solid walls and for an open jet is used.

In such equivalent homogeneous boundary conditions all details of the slot or perforation geometry are lost; in particular their orientation (longitudinal or transverse). Only bulk properties such as the porosity or open area ratio (OAR) are preserved. Wood(11) shows, for example, that the OAR for longitudinal slots would need to be less than 1% to achieve a boundary condition appreciably different from the open jet case. In practice, at such a small OAR, real fluid effects would be important, so a potential flow model for the cross-flow would be invalid. Moreover, Wood's analysis of this boundary condition indicates that only cross-flow velocities of order les than .5% of the mean flow would be in keeping with the linearizations involved in the derivation of this boundary condition.

III Previous Experimental Work

The results of conventional wall correction theories are shown compared with experiment (Lim (6)) on a 14% thick Clark-Y airfoil, of four different sizes, in the presence of longitudinally (streamwise) slotted walls. In these and subsequent figures, C is the airfoil chord and H is the wind tunnel test section height, or equivalent height, for two-dimensional testing (Figure 1). Figures 2,3,4,5 are taken from Parkinson and Lim (7).

Figure 2 shows the ratio of measured lift curve slope m to its value m_o in free air, as a function of model size C/H for longitudinally slotted walls of OAR 0.,5.6,11.1,18.5 and 100%. The agreement with the theory for longitudinal slots is good only for solid walls; that is, for zero OAR. All other walls were predicted to behave as if they were almost completely open. Thus the theory for longitudinally slotted walls is useless for predicting the behaviour of a model under actual test.

The same measured ratio of lift curve slopes is compared in Figure 3 with that predicted by porous wall theory (Woods (12)). This shows that the porosity parameter P (defined in Ref. 7) for a given wall OAR can be chosen to produce good agreement with the test data.

This result appears in Figure 4 to be true also for an airfoil with slotted flap, but the values of porosity parameter so obtained were not the same as for the basic airfoil, for the same wall configurations.

Figure 5 portrays the porosity parameter as a function of the wall OAR, which also depends on the model under test, an impossible situation for the practical use of porous wall theory.

IV Formulation of an Exact Theory

What then is needed is an exact (rather than a linearized) theory, where the net corrections to measured forces and moments are achieved directly, rather than additively. The method used in this investigation is an extension of the surface singularity distribution theory of A.M.O. Smith (8).

In Smith's method, the airfoil is represented by a distribution of sources and vortices around its perimeter. The velocities at points in the flow field due to all such sources and vortices are calculated directly. The usual flow boundary condition of zero flow through the airfoil surface is applied and a finite-velocity Kutta condition is applied at the trailing edge.

Again ϕ is the disturbance velocity potential which satisfies Laplace's equation, vanishes at infinity, and satisfies the appropriate boundary conditions on the airfoil.

The potential at a point P due to a single three-dimensional source singularity at a point Q is

$$\phi_P = \frac{-m}{4\pi} \frac{1}{r_{PQ}} \tag{1}$$

where m is the volume flow rate of fluid emitted by the source, and r_{PQ} is the distance between the points P and Q. The total potential due to all such sources distributed over an arbitrary surface S is

$$\phi_P = -\iint_S \frac{\sigma(Q)}{r_{PQ}} dS \tag{2}$$

where $\sigma(Q)$ is the source strength density, including the factor $1/4\pi$, of the source element at Q.

Since the disturbance velocity is the gradient of ϕ, the normal-velocity boundary condition at a surface can be expressed as

$$\frac{\partial \phi}{\partial n} = -\bar{V}_\infty \cdot \bar{n} + F \tag{3}$$

where $\bar{n}$ is the outward surface normal, $\bar{V}_\infty$ the undisturbed flow at upstream infinity, and F the value the normal velocity must take at the airfoil surface. F is zero for a solid (impermeable) boundary, but nonzero for suction or blowing there.

Analysis (Smith(8)) shows that the normal velocity contributions at P on S by such source elements dS consist of a "local" term,

$$2\pi\sigma(P) \tag{4}$$

due to the source element at P, plus a "far field" term

$$-\iint_S \frac{\partial}{\partial n}\left(\frac{1}{r_{PQ}}\right)\sigma(Q)dS \tag{5}$$

due to the summation of all other source elements Q on S. The resulting boundary condition

$$2\pi\sigma(P) - \iint_S \frac{\partial}{\partial n}\left(\frac{1}{r_{PQ}}\right)\sigma(Q)dS = -\bar{V}_\infty \cdot \bar{n} + F \tag{6}$$

comprises a Fredholm integral equation of the second kind, for the unknown continuous source strength density distribution

function $\sigma(P)$. Existence and uniqueness theorems for such equations may be found in Kellogg(5). The surface S may be disjoint, but the outward normal vector must be a continuous function of position.

In practice an approximating polygonal surface is used to represent a three-dimensional body so that the continuous distribution of sources becomes a succession of N finite distributed source elements. The normal-flow boundary condition is applied at a single "control point" on each source element.

Thus the resulting exact integral equation reduces to a set of N simultaneous linear algebraic equations for the strengths of N finite surface source elements.

Defining the linear operator

$$A_{ji} = -\iint_{S_j} \frac{\partial}{\partial n_j}\left(\frac{1}{r_{ji}}\right) dS_j \qquad (7)$$

the boundary condition applied at the i-th control point

$$\sum_{j=1}^{N} A_{ji}\sigma_j = -\bar{V}_\infty \circ \bar{n}_i + F_i \qquad (8)$$

indicates A_{ji} to be the normal velocity induced at control point 'i' by a unit strength source element at 'j'. Hence A_{ii} is 2π for all i=1,2,...N.

For a two-dimensional airfoil this approximating surface becomes a polygonal cylinder. A Kutta condition is applied at the two control points adjacent to the trailing edge - this fixes the net circulation about the airfoil.

With respect to Cartesian axes x_j and y_j fixed to the j-th

source element (Figure 6), the integration of a two-dimensional line source into a two-dimensional distributed source element produces at a point 'i' velocity components

$$V_{x_j} = \frac{\partial \phi_{ji}}{\partial x_j} = \log \left\{ \frac{\left(x_j + \frac{\Delta s_j}{2}\right)^2 + y_j^2}{\left(x_j - \frac{\Delta s_j}{2}\right)^2 + y_j^2} \right\} \tag{9}$$

and

$$V_{y_j} = \frac{\partial \phi_{ji}}{\partial y_j} = 2\tan^{-1}\left\{ \frac{y_j \Delta s_j}{x_j^2 + y_j^2 - \left(\frac{\Delta s_j}{2}\right)^2} \right\} \tag{10}$$

where x_j and y_j are the distances from the j-th to the i-th element; the j-th element has length Δs_j.

With reference to Cartesian "wind axes" X and Y, (X is in the wind direction), the j-th source element is inclined at an angle θ_j to the X-axis. Thus

$$A_{ji} = V_{y_j}\cos(\theta_i - \theta_j) - V_{x_j}\sin(\theta_i - \theta_j) \tag{11}$$

and its orthogonal partner

$$B_{ji} = V_{x_j}\cos(\theta_i - \theta_j) + V_{y_j}\sin(\theta_i - \theta_j) \tag{12}$$

are the normal and tangential disturbance velocities respectively at control point 'i' due to a unit strength source element at 'j'.

Corresponding expressions for the velocity components due to a distributed vortex element of circulation strength density $\gamma(Q)$ can be obtained. Then the normal and tangential velocities at control point 'i' due to all N source and vortex elements and the uniform approach flow U are

$$V_{n_i} = \sum_{j=1}^{N} A_{ji}\sigma_j - \sum_{k=1}^{N} B_{ki}\gamma_k - U\sin\theta_i \qquad (13)$$

and

$$V_{t_i} = \sum_{j=1}^{N} B_{ji}\sigma_j + \sum_{k=1}^{N} A_{ki}\gamma_k + U\cos\theta_i \qquad (14)$$

Hence the normal-flow boundary condition becomes, for zero F_i,

$$V_{n_i} = 0 \qquad (15)$$

at all N control points, while the finite-velocity Kutta condition becomes

$$V_{t_{upper}} = -V_{t_{lower}} \qquad (16)$$

at the two control points adjacent to the airfoil trailing edge.

In practice, all vortex elements on a closed body requiring a Kutta condition are chosen of equal strength γ, so the flow about an N-sided polygonal airfoil requires the solution of N+1 equations in the N+1 unknowns $\sigma_1, \sigma_2, \ldots \sigma_N$ and γ. Usually the solution is obtained directly by the method of Gauss-elimination, although indirect iterative procedures are also possible.

In the present investigation, the above method of distributed singularities is extended to include multiple-element airfoils in the presence of solid or slotted wind tunnel walls. On solid wall sections, only the zero normal-velocity condition applies, hence only source elements are applied there. On airfoil-shaped bodies with Kutta conditions applied at their

individual trailing edges, both source and vortex elements are required. Thus for the two-dimensional configuration of Figure 7, the system of N+M equations to be solved is composed of the N equations

$$\sum_{j=1}^{N} A_{ji}\sigma_j - \sum_{k=1}^{M}\gamma_k \sum_{m=1}^{R(k)} B_{mi} = U\sin\theta_i \qquad i=1,2,\cdots N \tag{17}$$

prescribing zero normal velocities, and the M equations

$$\sum_{j=1}^{N}(B_{ju_s}+B_{jL_s})\sigma_j + \sum_{k=1}^{M}\gamma_k \sum_{m=1}^{R(k)}(A_{mU_s}+A_{mL_s}) = -U(\cos\theta_{U_s}+\cos\theta_{L_s})$$

$$s=1,2,\cdots M \tag{18}$$

for the M bodies with Kutta conditions at their trailing edges. The subscripts U and L indicate the control points on the upper and lower surfaces of an airfoil section, at the trailing edge.

Thus there are:

-a total of N source elements distributed over the airfoils and solid walls.

-a total of M bodies requiring Kutta conditions.

-a total of $\sum_{k=1}^{M} R(k)$ vortex elements distributed over the airfoils; the k-th such body has R(k) source elements and R(k) equal-strength vortex elements distributed over it.

-N unknown source strength densities σ_j.

-M unknown vortex strength densities γ_k.

-N+M equations in the N+M unknowns $\sigma_1, \sigma_2, \ldots, \sigma_N, \gamma_1, \gamma_2, \ldots, \gamma_M$.

V Numerical Solution

A program written in FORTRAN for use on the UBC IBM 360/67 computer is used to construct the matrices A_{ji} and B_{ji}, given the coordinates, lengths and orientations of the source and vortex elements on the airfoil and walls. These matrices are then used to assemble the coefficients of the unknowns in the N+M equations. Typically N+M is of order 300 to 400, hence the matrices A_{ji} and B_{ji} each contain more than 100,000 nonzero, nonsymmetric entries. The total computational capacity of the 360/67 is only 250,000 entries, hence such large matrices must be partitioned for computation and temporary storage on auxiliary devices; for example, on magnetic tapes or discs. The matrices A_{ji} and B_{ji} describe the relative geometry of the source and vortex elements; that is, their relative position and orientation. These matrices must be recalculated for each change in relative geometry.

The system of equations to be solved is written

$$
\begin{aligned}
&c_{1,1}\sigma_1 + c_{2,1}\sigma_2 + \cdots + c_{N,1}\sigma_N + c_{N+1,1}\gamma_1 + \cdots + c_{N+M,1}\gamma_M = d_1 \\
&c_{1,2}\sigma_1 + c_{2,2}\sigma_2 + \cdots + c_{N,2}\sigma_N + c_{N+1,2}\gamma_1 + \cdots + c_{N+M,2}\gamma_M = d_2 \\
&\qquad\vdots \\
&c_{1,N}\sigma_1 + c_{2,N}\sigma_2 + \cdots + c_{N,N}\sigma_N + c_{N+1,N}\gamma_1 + \cdots + c_{N+M,N}\gamma_M = d_N \\
&c_{1,N+1}\sigma_1 + c_{2,N+1}\sigma_2 + \cdots + c_{N,N+1}\sigma_N + c_{N+1,N+1}\gamma_1 + \cdots + c_{N+M,N+1}\gamma_M = d_{N+1} \\
&\qquad\vdots \\
&c_{1,N+M}\sigma_1 + c_{2,N+M}\sigma_2 + \cdots + c_{N,N+M}\sigma_N + c_{N+1,N+M}\gamma_1 + \cdots + c_{N+M,N+M}\gamma_M = d_{N+M}
\end{aligned}
\qquad (19)
$$

where the matrix C_{ji} and the column vector d in the system $C(\sigma;\gamma)=d$ are assembled from the matrices A_{ji} and B_{ji} by means of

equations (17) and (18); that is,

$$C_{ji} = \begin{cases} A_{ji} & j=1,2,\cdots N;\ i=1,2,\cdots N \\ -\sum_{m=1}^{R(k)} B_{mi} & k=1,2,\cdots M;\ j=N+k;\ i=1,2,\cdots N \\ B_{jU_s} + B_{jL_s} & j=1,2,\cdots N;\ s=1,2,\cdots M;\ i=N+s \\ \sum_{m=1}^{R(k)} (A_{mU_s} + A_{mL_s}) & k=1,2,\cdots M;\ j=N+k;\ s=1,2,\cdots M;\ i=N+s \end{cases} \tag{20}$$

and

$$d_i = \begin{cases} U\sin\theta_i & i=1,2,\cdots N \\ -U\cos\theta_{U_s} - U\cos\theta_{L_s} & s=1,2,\cdots M;\ i=N+s \end{cases} \tag{21}$$

The summations

$$V_{n_i} = \sum_{j=1}^{N'} A_{ji}\sigma_j - \sum_{k=1}^{M}\gamma_k \sum_{m=1}^{R(k)} B_{mi} - U\sin\theta_i \tag{22}$$

and

$$V_{t_i} = \sum_{j=1}^{N} B_{ji}\sigma_j + \sum_{k=1}^{M}\gamma_k \sum_{m=1}^{R(k)} A_{mi} + U\cos\theta_i \tag{23}$$

provide the net normal and tangential velocities at control points 'i' due to all sources and vortices 'j'. At all control points on solid surfaces, V_{n_i} is zero, and the local pressure coefficient C_{p_i} is calculated from V_{t_i}.

$$C_{p_i} = 1 - \left(\frac{V_{t_i}}{U}\right)^2 \tag{25}$$

The resulting values of C_{p_i} may be integrated numerically around the airfoil contour to determine the lift, drag, and

pitching moment coefficients, from the expressions

$$C_{L_T} = -\frac{1}{C}\sum_i C_{p_i}\Delta x_i$$

$$C_{D_T} = \frac{1}{C}\sum_i C_{p_i}\Delta y_i$$

$$C_{M_{o_T}} = \frac{1}{C^2}\sum_i C_{p_i}(x_i\Delta x_i + y_i\Delta y_i) \qquad (26)$$

where

$$\Delta x_i = \Delta s_i \cos\theta_i \ , \quad \Delta y_i = \Delta s_i \sin\theta_i \qquad (27)$$

and summations are performed clockwise around the polygonal contours.

Resultant velocities may also be calculated at points in the flow field not on the airfoil or walls, so that streamlines throughout the flow field may be drawn as isoclines.

VI Results

The agreement of pressure distributions calculated by Smith's method, for airfoils in free air, with two-dimensional tests is well established (Smith(8)). Figure 8 shows a comparison of calculated pressure distributions for a 14% thick Clark-Y airfoil in free air and in the presence of solid walls. The walls, for this size model, produce 30% higher lift.

Figure 9 shows a comparison of an experimentally determined pressure distribution for an NACA 23012 airfoil with flap (Wenzinger et al(10)), with calculated pressure distributions for the same airfoil in free air and in the presence of solid walls. Experimentally, the potential flow free-air pressures are not achieved because of boundary layer effects.

For both the above airfoils, an important observation is that the undersurface pressure does not change much in the presence of solid walls; hence the upper or suction surface provides most of the increased lift.

The lift coefficients are reported in terms of the lift coefficient C_{L_T} developed by the airfoil in the tunnel and C_{L_F} developed in free air.

Figure 10 shows the variation of C_{L_T} with angle of attack α for models of differing C/H. For small models, the lift curves are concave downward as is usual, while for large models they are concave upward.

The ratio of lift coefficients is shown in Figure 11 as a

function of model size, for three angles of attack. The corresponding prediction of conventional solid wall theory (Woods(12)), which is independent of angle of attack, agrees well with the test data (Lim(6)).

The very large corrections for large airfoils developing high lift, shown in the above results, prompted a search for a wall configuration that would exhibit the known cancelling effects of partly open, partly closed walls, and which would therefore provide negligible or small wall corrections.

The first configuration investigated was a set of multiple airfoils in an otherwise uniform stream of infinite extent (Figure 12). This configuration might be used to represent a two-dimensional tunnel with transversely (spanwise) slotted walls. With airfoil-shaped transverse slats, no flow separation would occur at the slats, as each winglet would be operating in an unstalled condition, with a Kutta condition applied at its trailing edge.

Consider the limiting lower streamline AB, which enters the tunnel near the entrance to the test section. Physically, this lower streamline is a shear layer, idealized as a free streamline, at constant zero reference pressure, which brings turbulent mixing into the tunnel, close to the airfoil, an undesirable effect. But the corresponding streamline in the multiple airfoil-infinite stream representation is not a free streamline, but merely one of the infinite stream. Thus, in this representation, the pressure is not zero on this lower streamline, and errors would be introduced in representing the

flow in this manner; in particular, close to the underside of the airfoil.

Similarly the upper limiting streamline cannot be correctly represented easily, but since this streamline is separated from the airfoil by the intervening slats with their boundary conditions impressed on the flow, the errors in incorrect pressure and location in the representation of this streamline should have only secondary effects on the main airfoil.

With only one slotted wall, Figure 13, it should still be possible to produce the cancelling effects of partly open, partly closed walls, since the upper slotted wall is adjacent to the suction side of the airfoil, where most of the increased lift is developed. Hence a combination of a transversely slotted upper wall with a solid lower wall was envisaged as an effectively correction-free test configuration, for a lifting airfoil.

This configuration should be accurately represented by two-dimensional potential flow theory, since the flow angles at the wall slats should be small enough that these winglets will be unstalled, and the upper shear layer will re-enter the tunnel only well downstream of the airfoil.

An investigation of this configuration followed.

For the Clark-Y, at an angle α_{base} of 20°, Figure 14 shows the ratio of lift coefficients as a function of model size for a 50% and 75% OAR upper wall. Also shown are the curves for two solid walls, and for the airfoil in ground effect.

For the same airfoil at the same angle of attack, the ratio of lift coefficients in Figure 15 is shown as a function of upper wall OAR, for a range of model sizes. An upper wall of zero OAR corresponds to two solid walls; 100% OAR corresponds to the airfoil in ground effect. Where the ratio of lift coefficients is unity, there is zero net wall correction; this occurs for this airfoil at approximately 70% OAR.

The pressure distribution for the Clark-Y at an α_{base} of 20° for such a zero correction configuration of 70% OAR, with model size C/H of .72, appears in Figure 16 along with the corresponding pressure distribution for free air. The net lift is the same in both cases. Although there is less suction over the forward upper surface, there is increased suction over the rearward portion of the airfoil.

Similar results are shown in Figure 17 for the same airfoil but at a different α_{base} of 12°. Again a slotted upper wall of 70% OAR should provide a relatively correction-free test configuration. Comparison is also made with the theory for a circular arc airfoil in ground effect (Tomotika et al(9)) of similar 5.3% camber, but at an α_{chord} of 5°. The agreement is favourable.

Results obtained for the NACA 23012 with flap were similar. Figure 18 indicates that a transversely slotted upper wall of 70% OAR with a solid lower wall provides a relatively correction-free test configuration.

The relative error in C_{L_T} for a 70% upper wall OAR is shown

in Figure 19 for the Clark-Y airfoil at four angles of attack and the NACA 23012 airfoil with flap. The relative error at this OAR is less than 3%, except for extremely large models.

Table 1 outlines the details of all configurations tested.

VII Conclusion

An extension of the two-dimensional potential flow thoery based on the surface singularity distribution procedure has shown that a relatively correction-free wind tunnel test configuration for lifting airfoils can be achieved for a wide range in model sizes by utilizing a 70% open area ratio transversely (spanwise) slotted upper wall, in conjunction with a solid lower wall. Small or negligible corrections can be achieved for a wide range of angles of attack, and for different models, that is, single airfoils or airfoil-flap combinations. A program of experimental verification of these results should be undertaken. Where the wall corrections are not negligible but small, a linearized perturbation theory based on this configuration might be developed.

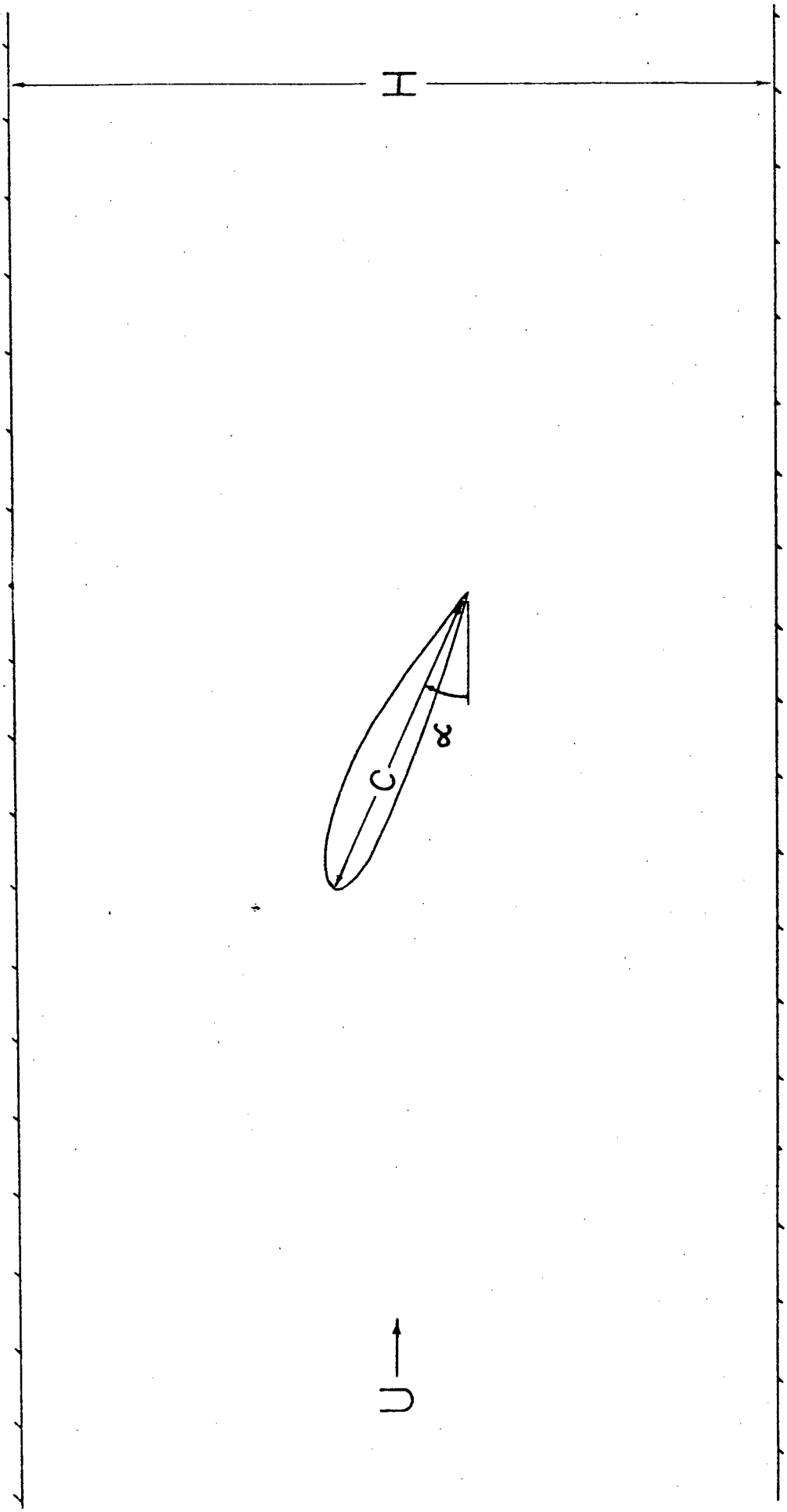

Figure 1. Airfoil in a wind tunnel.

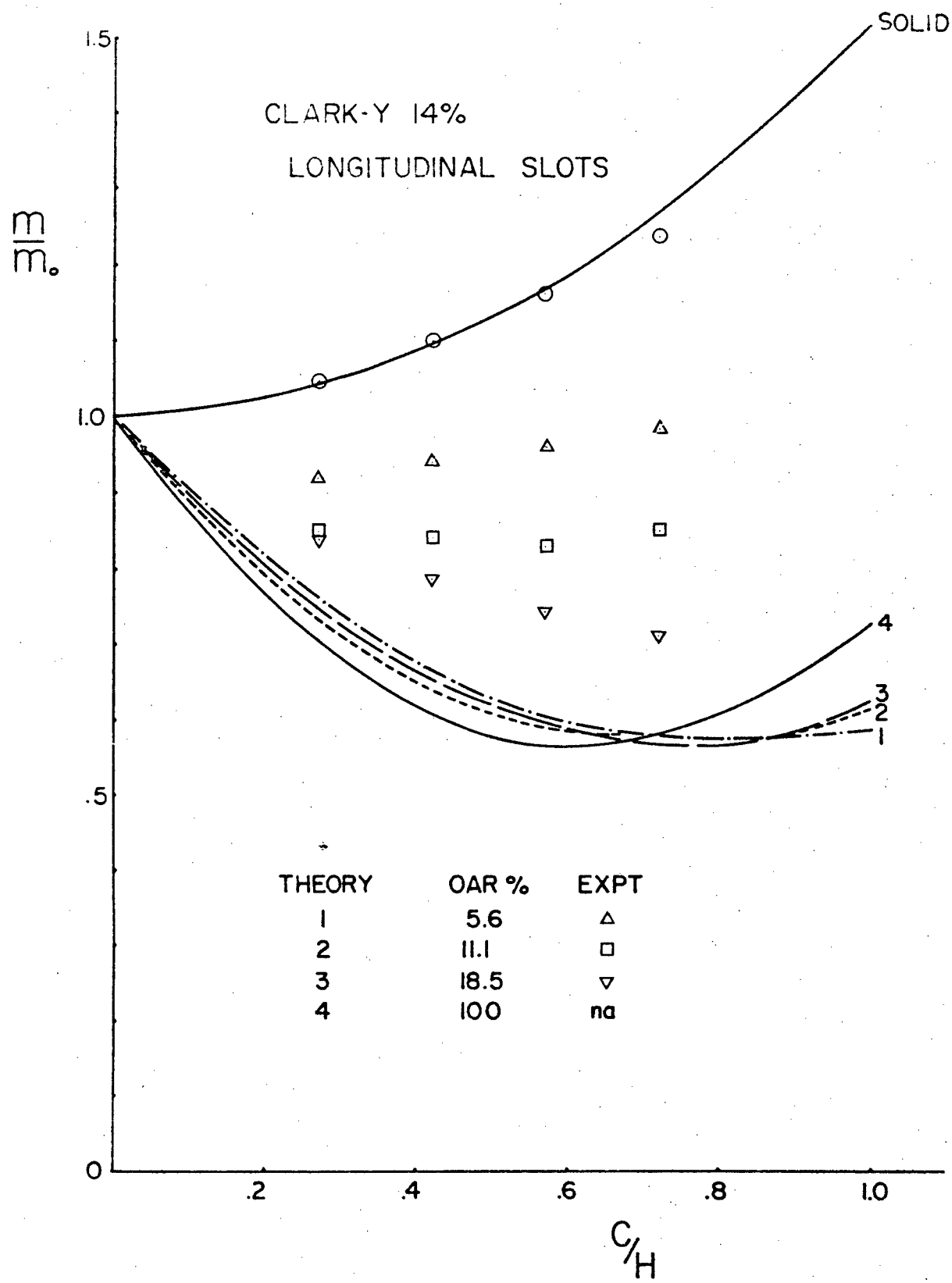

Figure 2. Comparison of longitudinally slotted wall lift theory with data for Clark-Y airfoil.

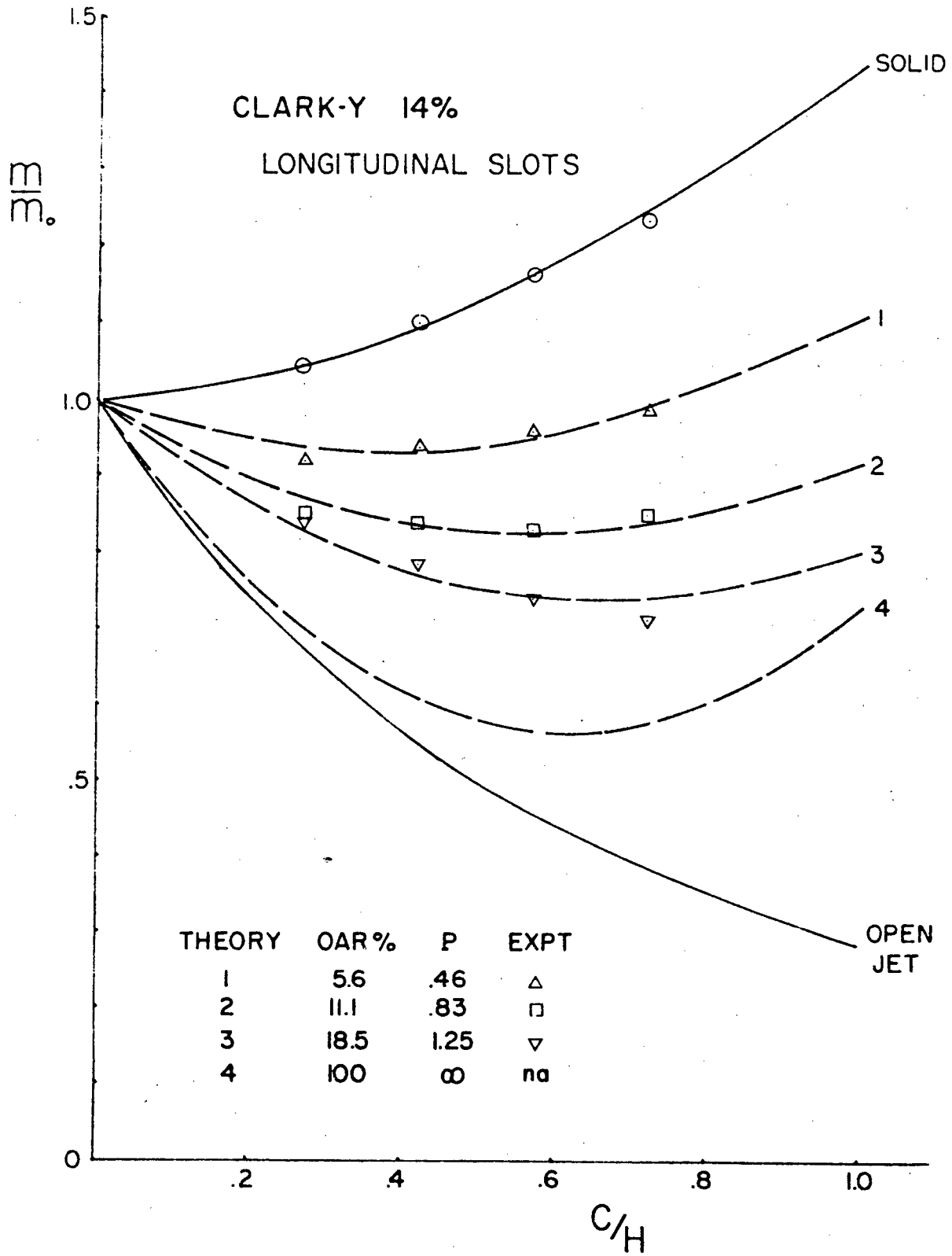

Figure 3. Comparison of porous-wall lift theory with data for Clark-Y airfoil tested between longitudinally slotted walls.

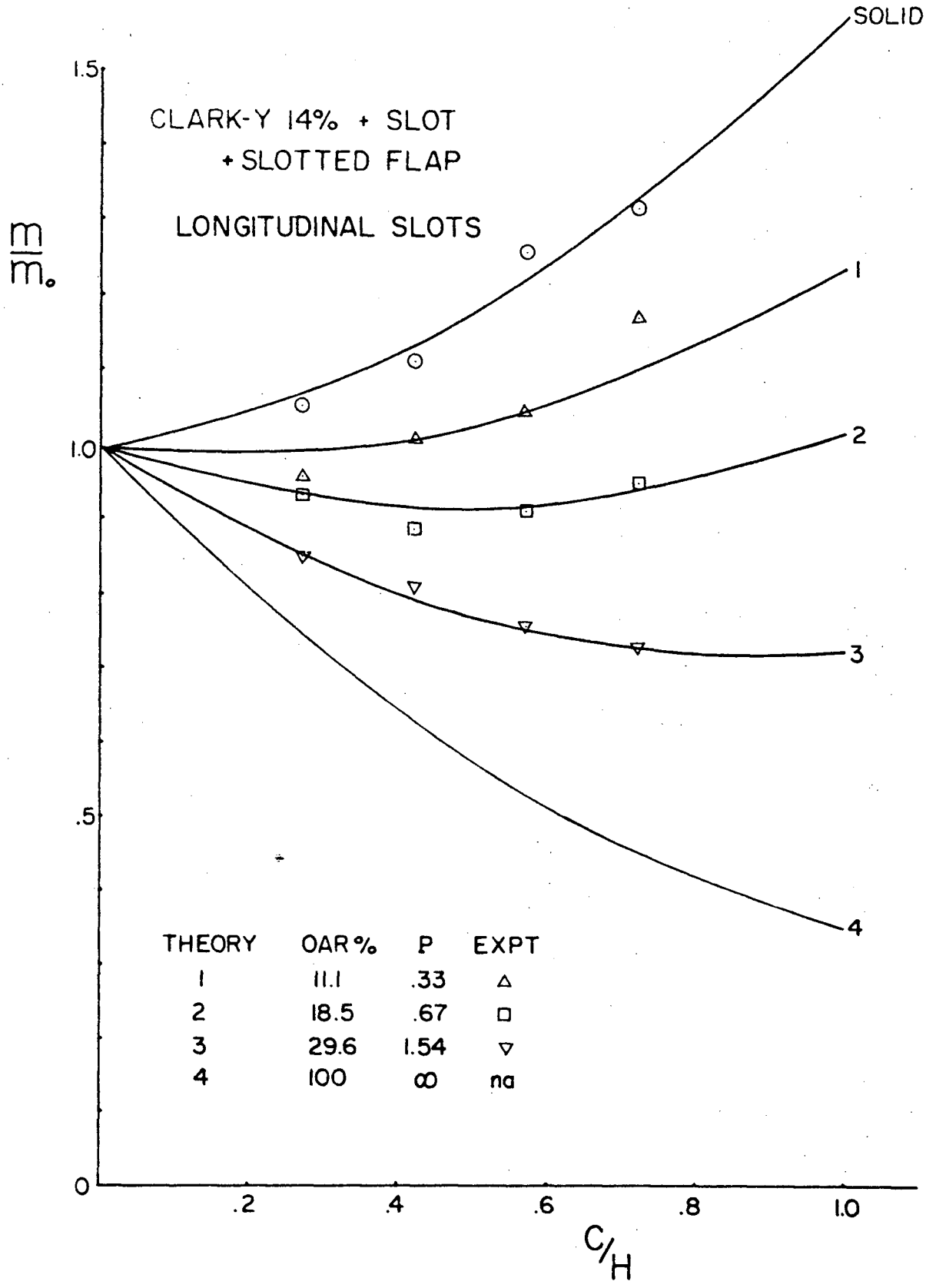

Figure 4. Comparison of porous-wall lift theory with data for Clark-Y airfoil with slotted flap tested between longitudinally slotted walls.

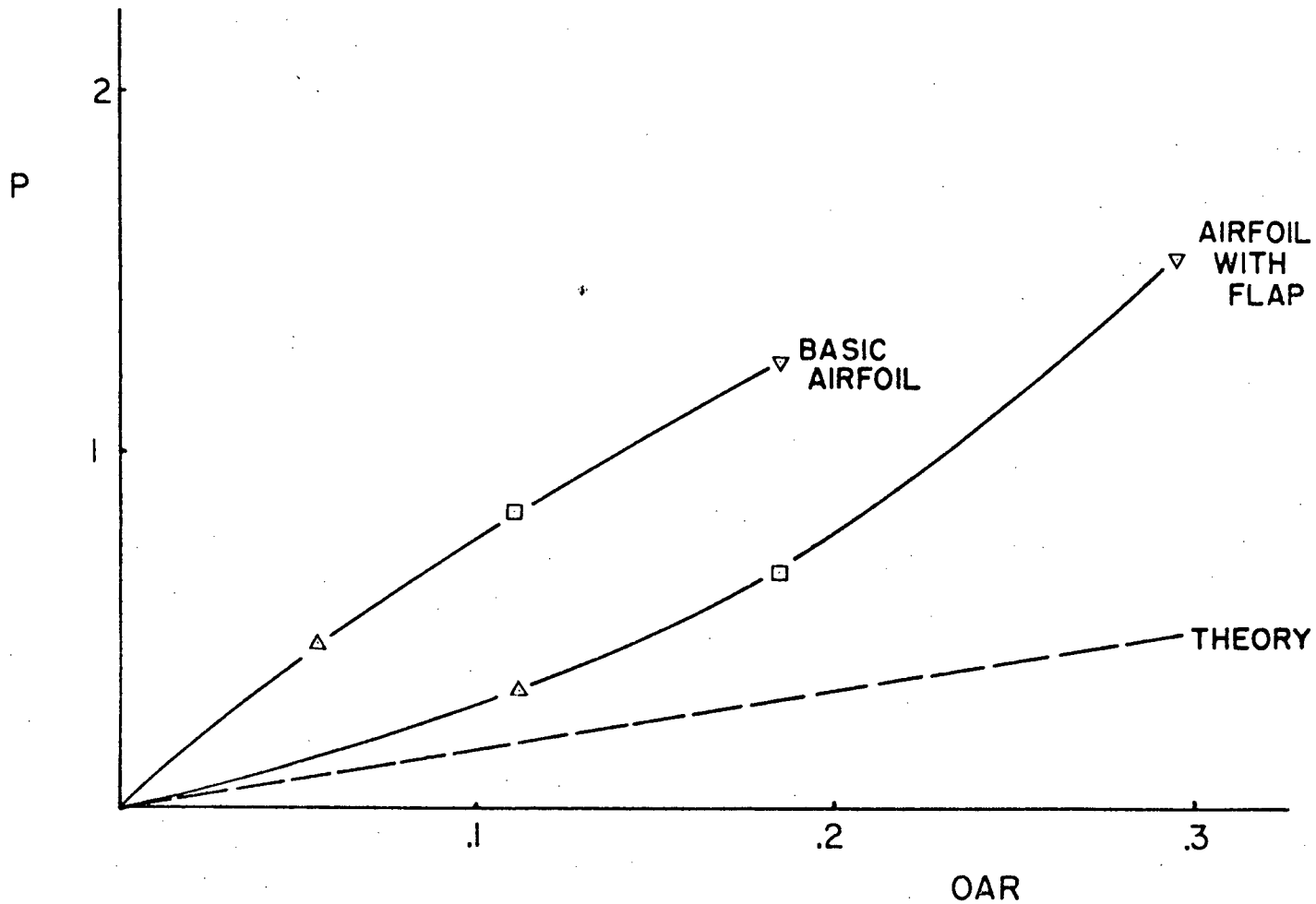

Figure 5. Porosity parameter as a function of open-area ratio.

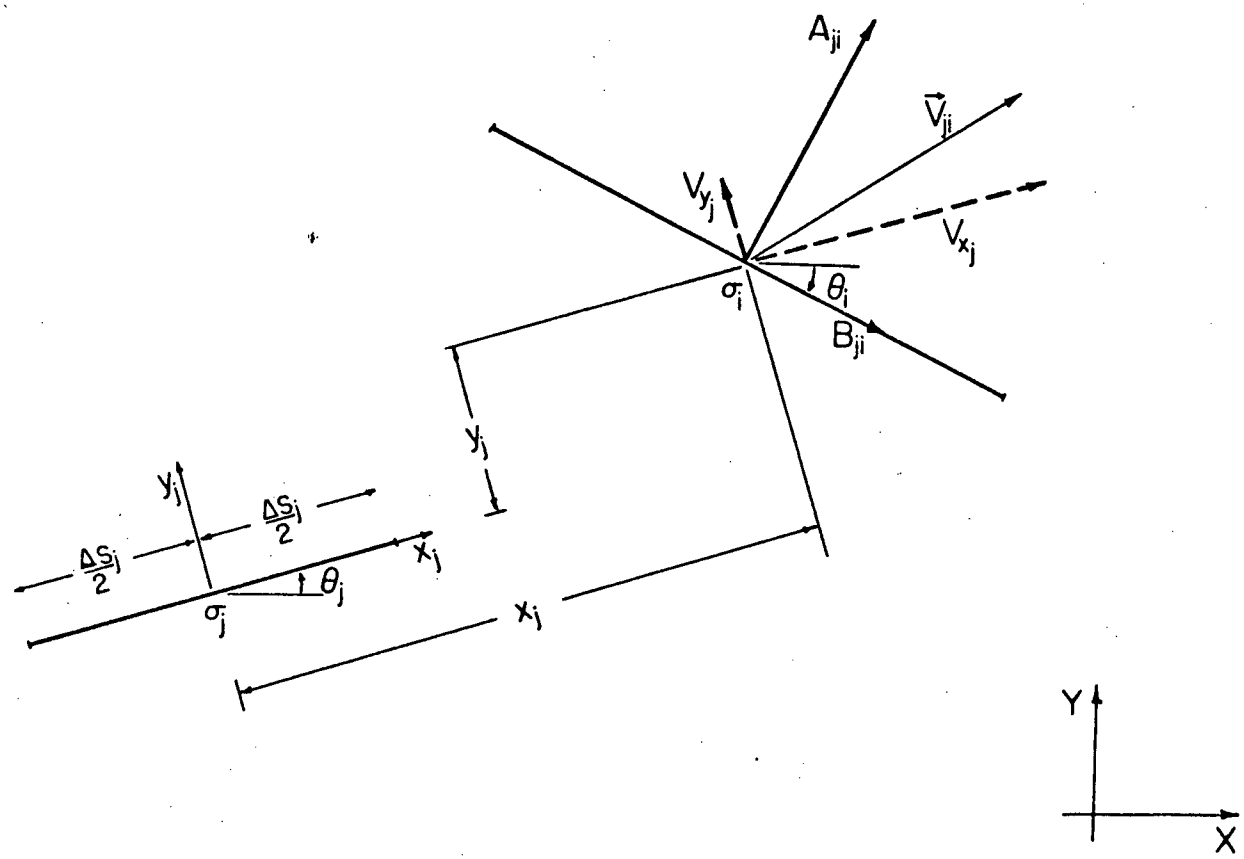

Figure 6. Geometry and notation for Smith's method.

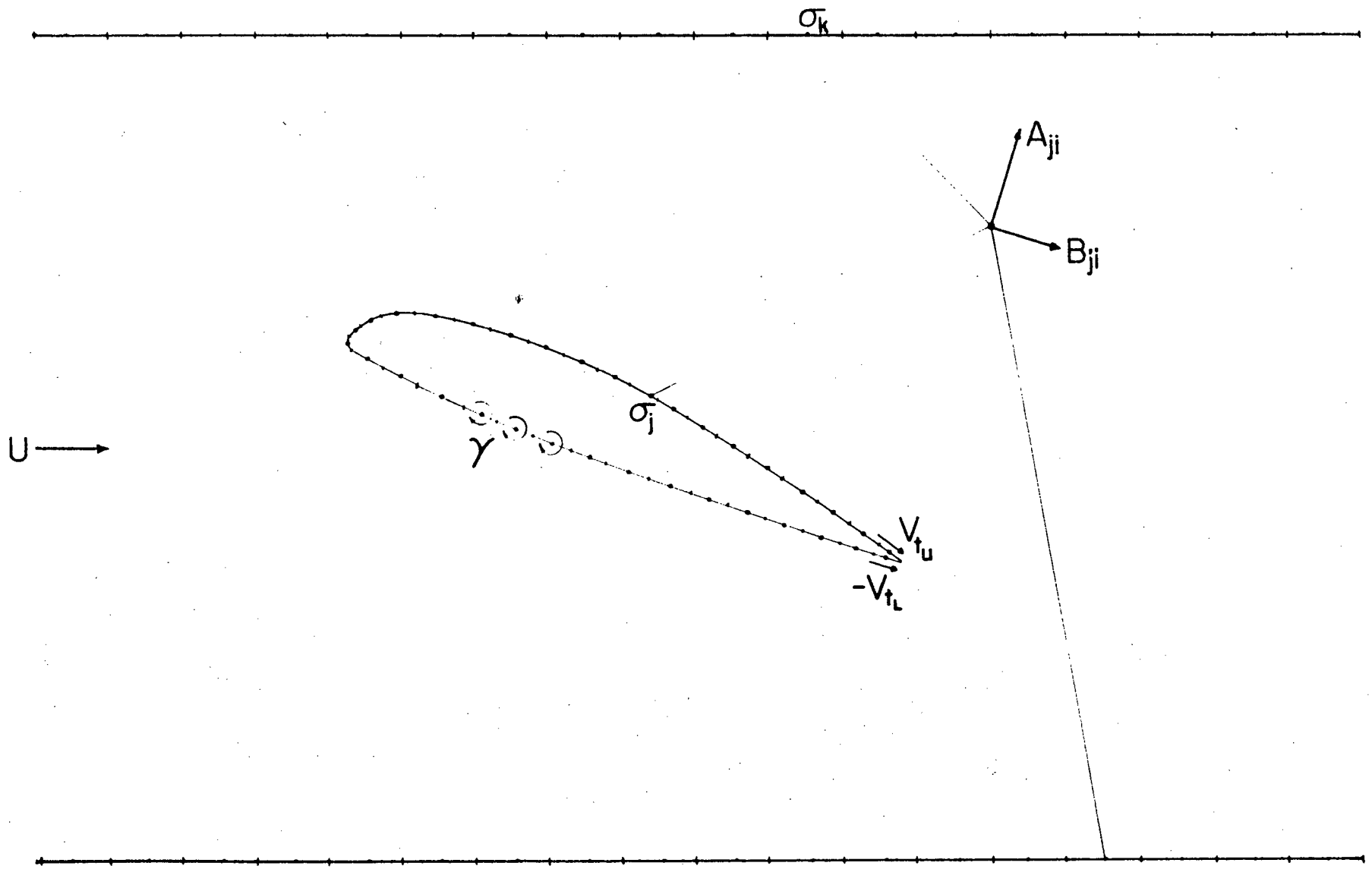

Figure 7. Source and vortex distributions for a two-dimensional airfoil between solid walls.

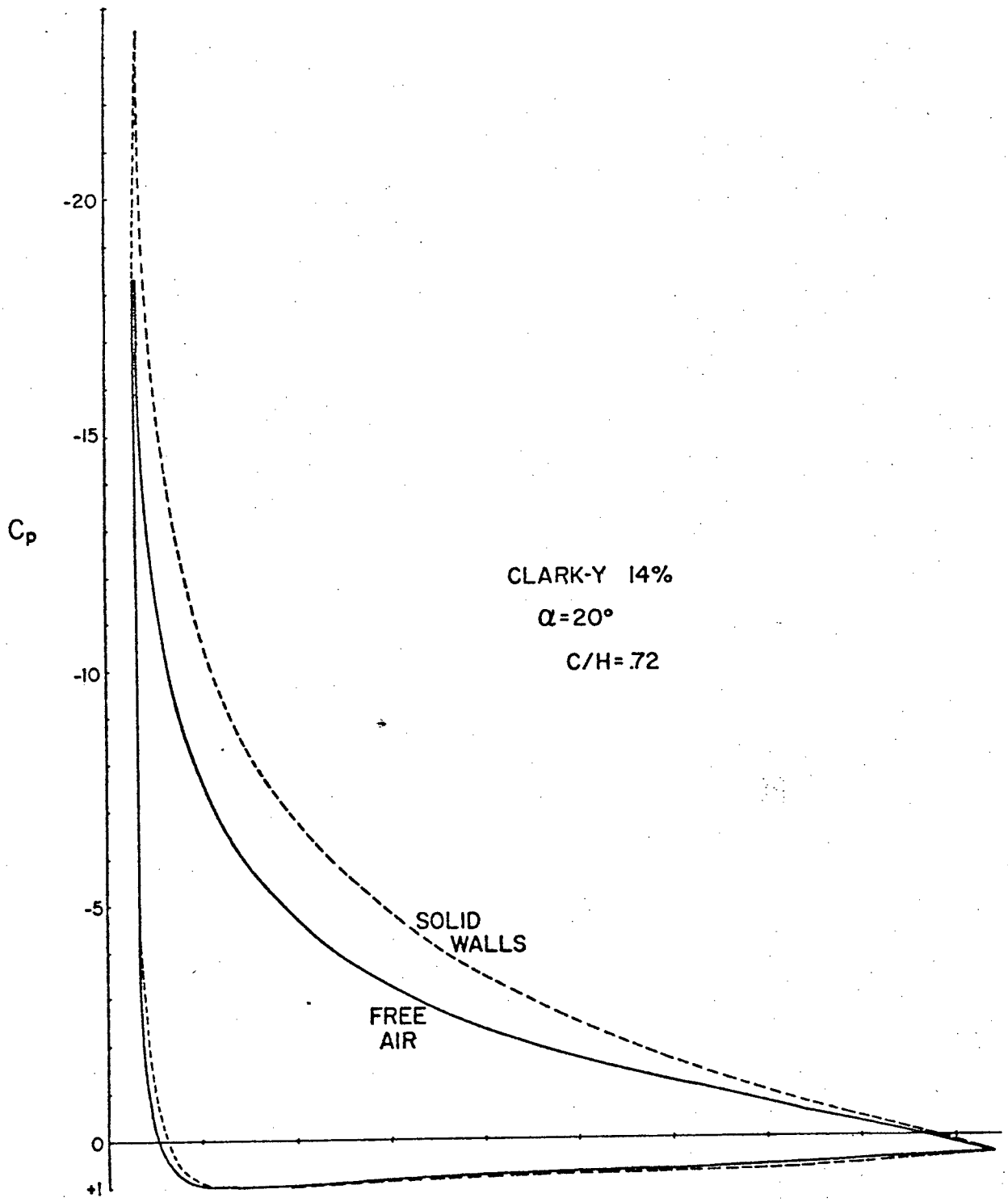

Figure 8. Pressure distributions for Clark-Y airfoil.

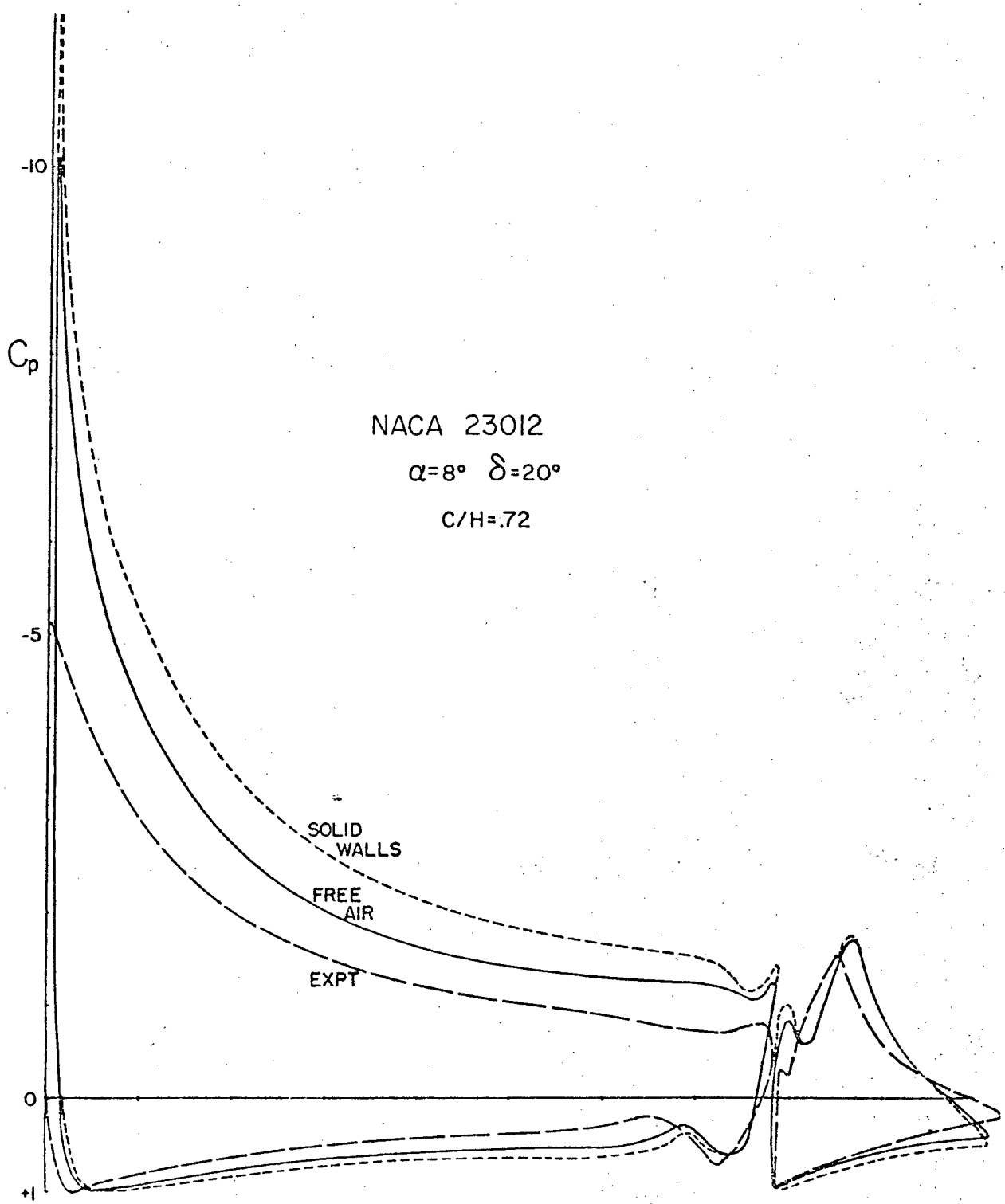

Figure 9. Pressure distributions for NACA 23012 airfoil.

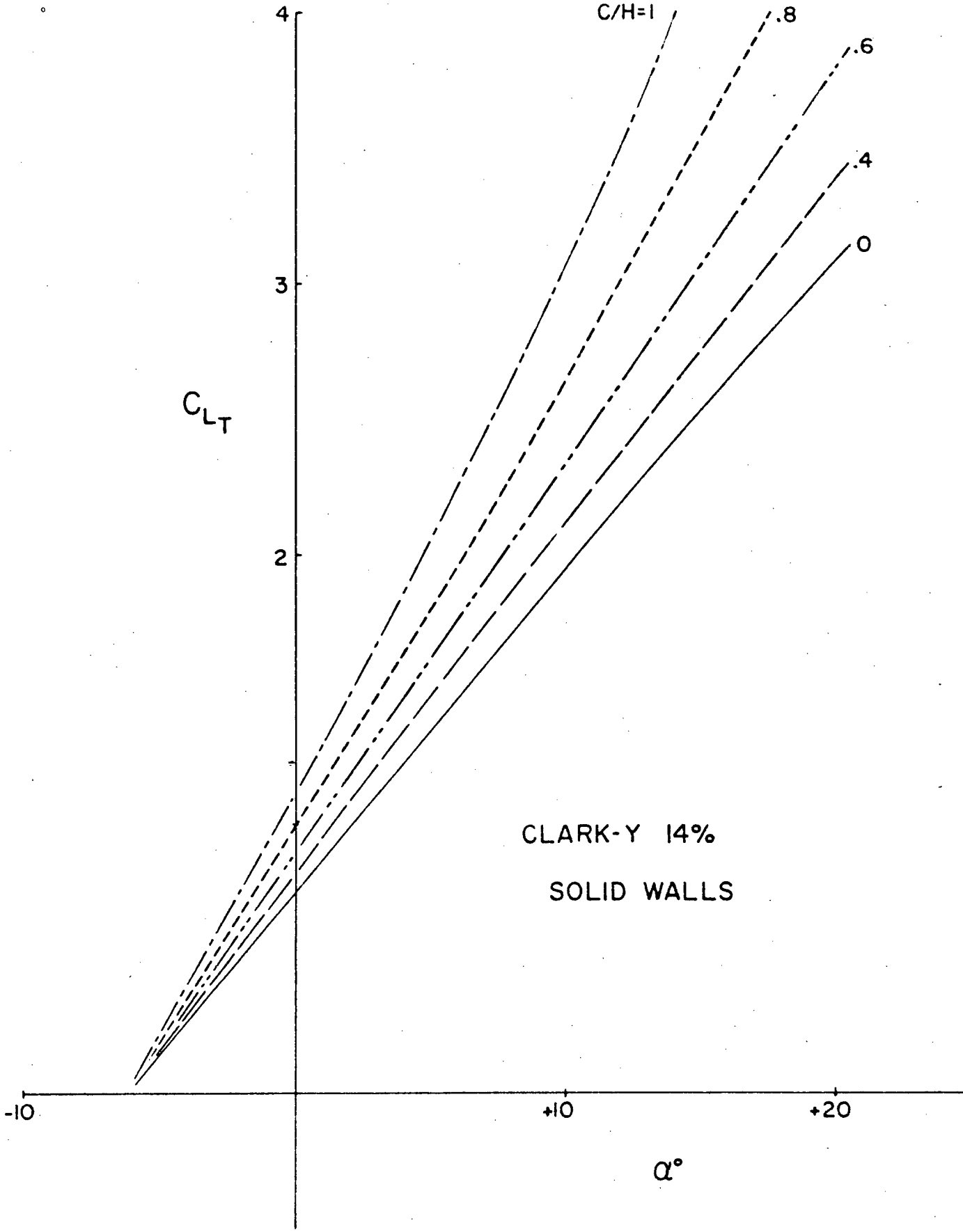

Figure 10. Lift coefficient for Clark-Y airfoil between solid walls.

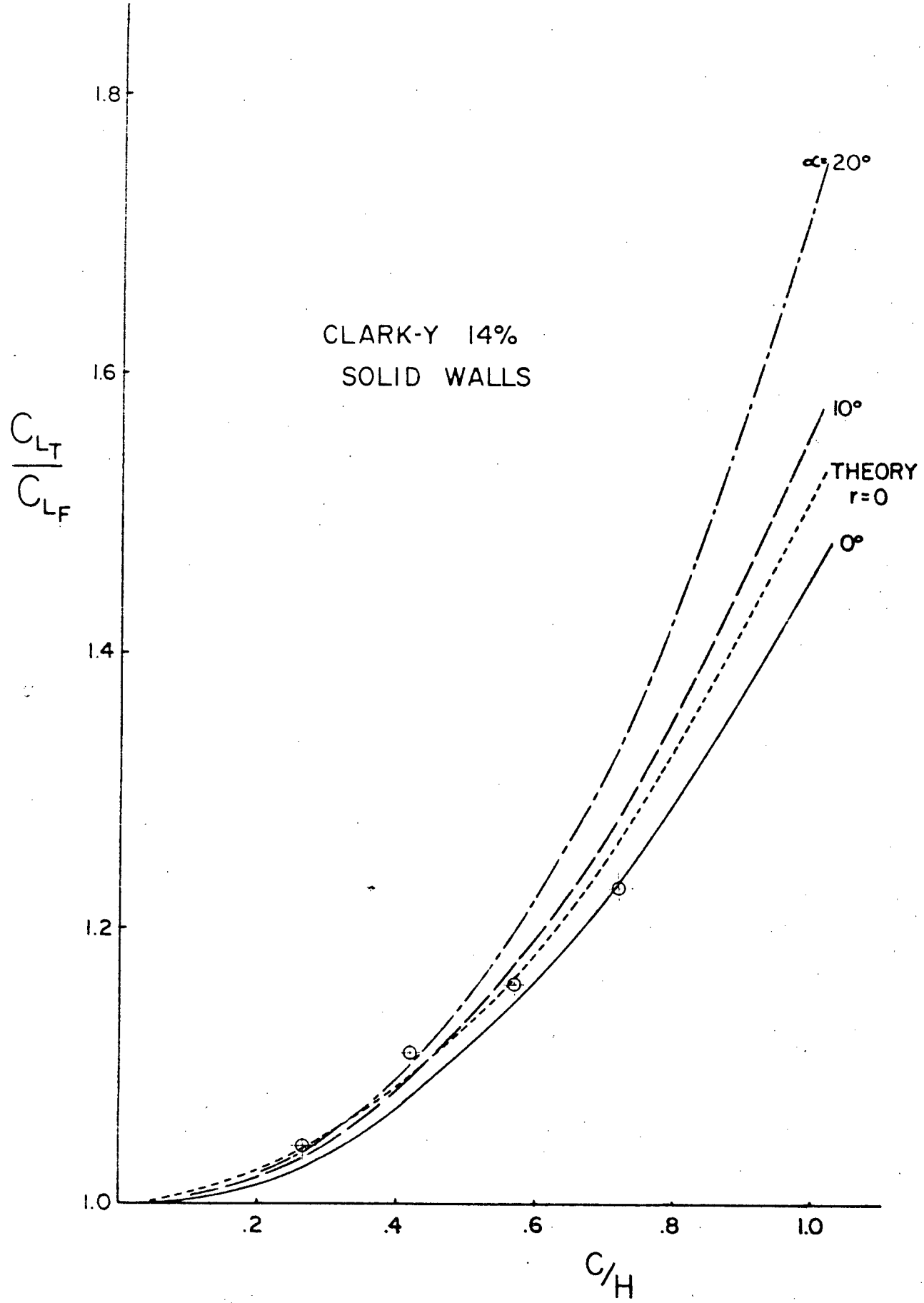

Figure 11. Ratio of lift coefficients for Clark-Y airfoil between solid walls.

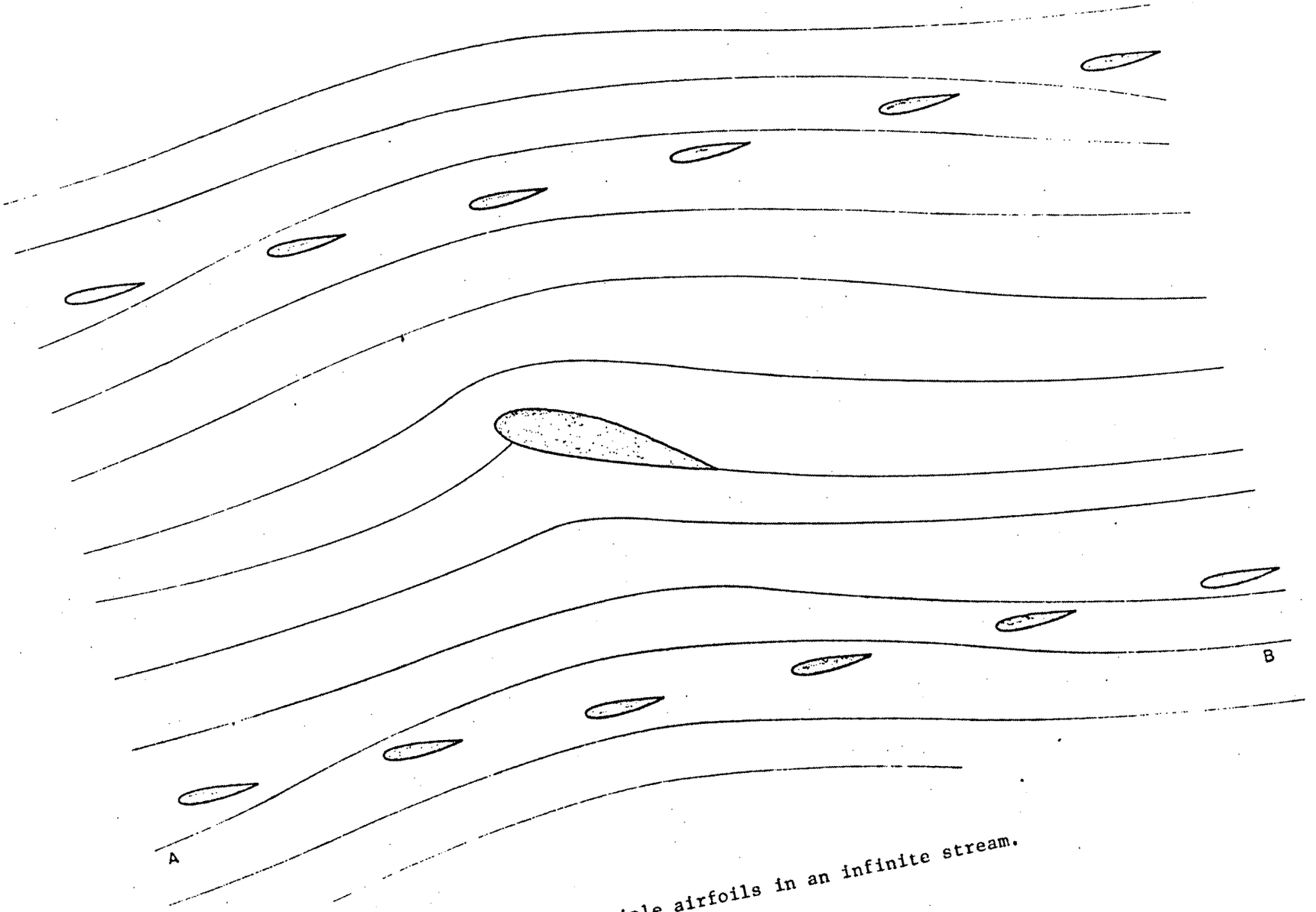

Figure 12. Streamlines for a set of multiple airfoils in an infinite stream.

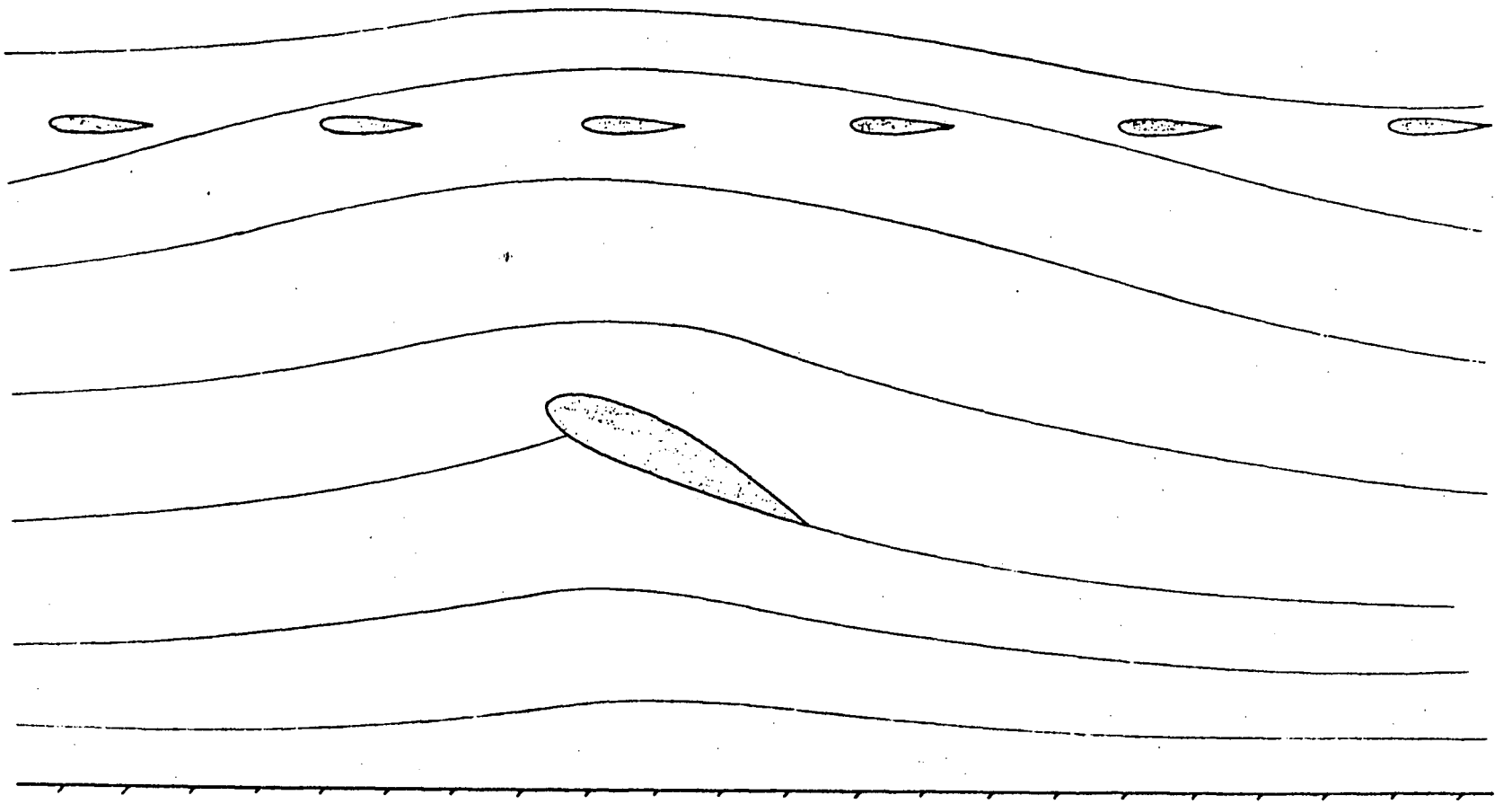

Figure 13. Streamlines for an airfoil between transversely slotted upper and solid lower walls.

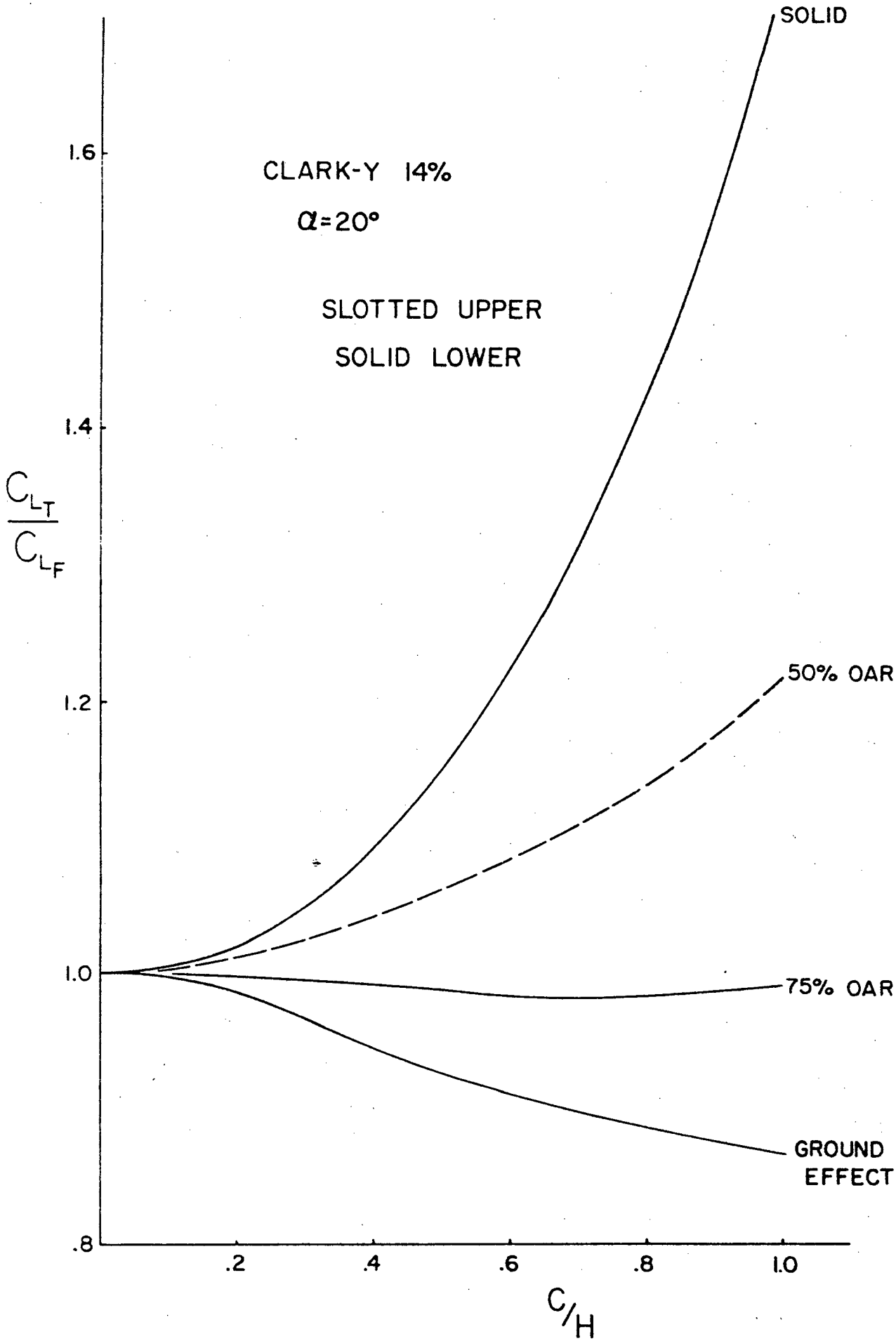

Figure 14. Variation of lift coefficient ratio with wall geometry for Clark-Y airfoil.

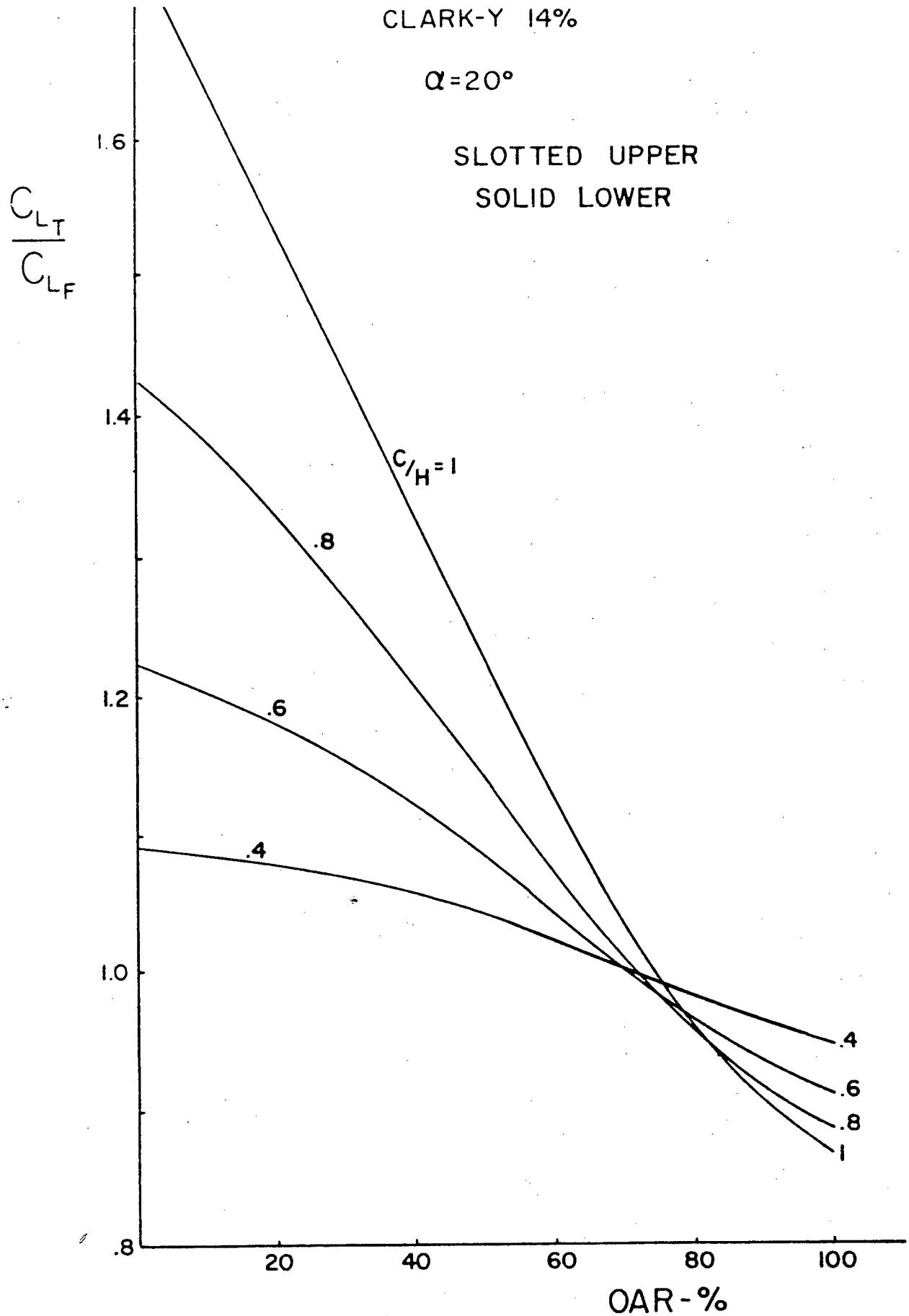

Figure 15. Variation of lift coefficient ratio with upper wall open-area ratio for Clark-Y airfoil.

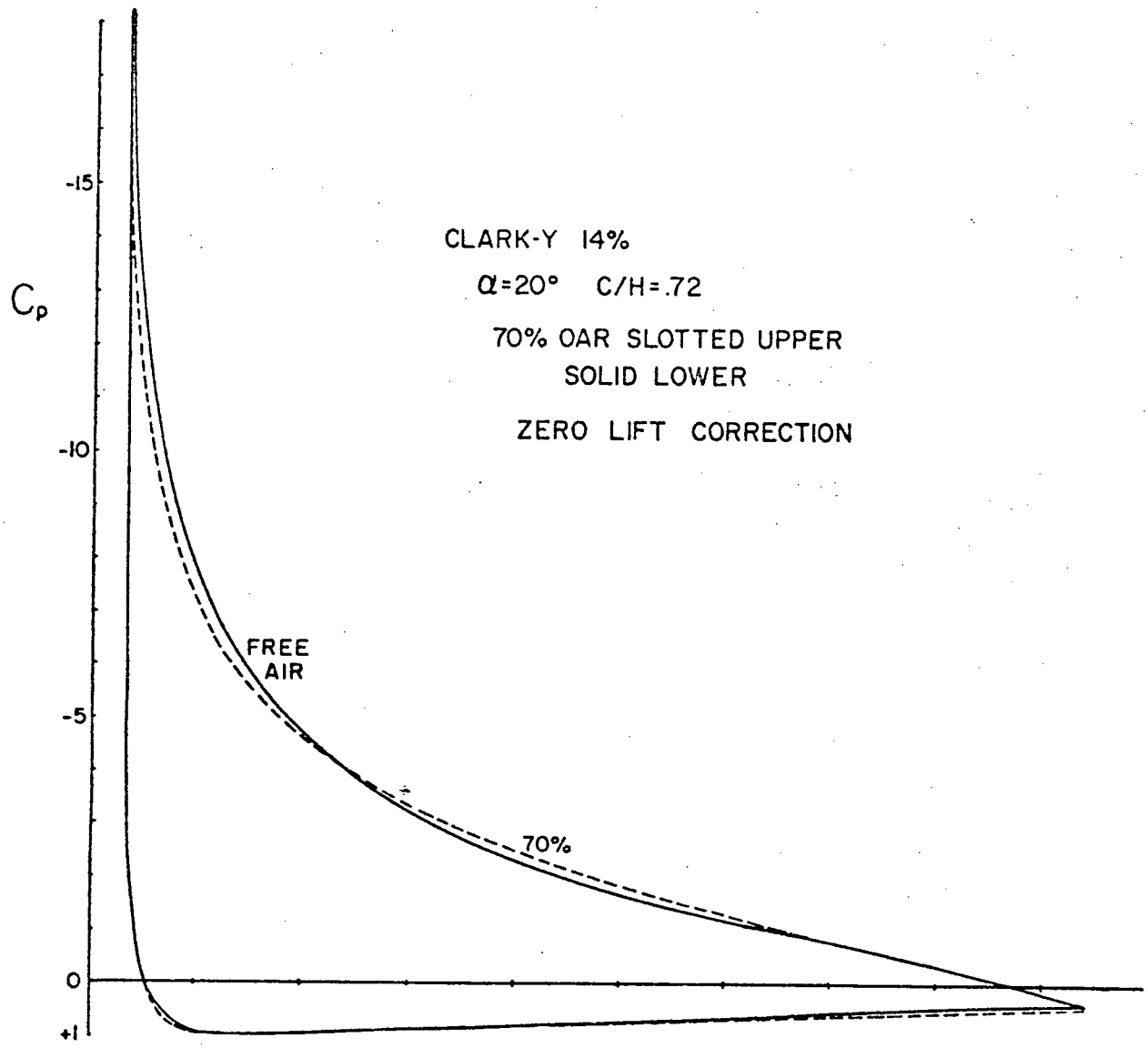

Figure 16. Pressure distribution for Clark-Y airfoil in correction-free lift test configuration.

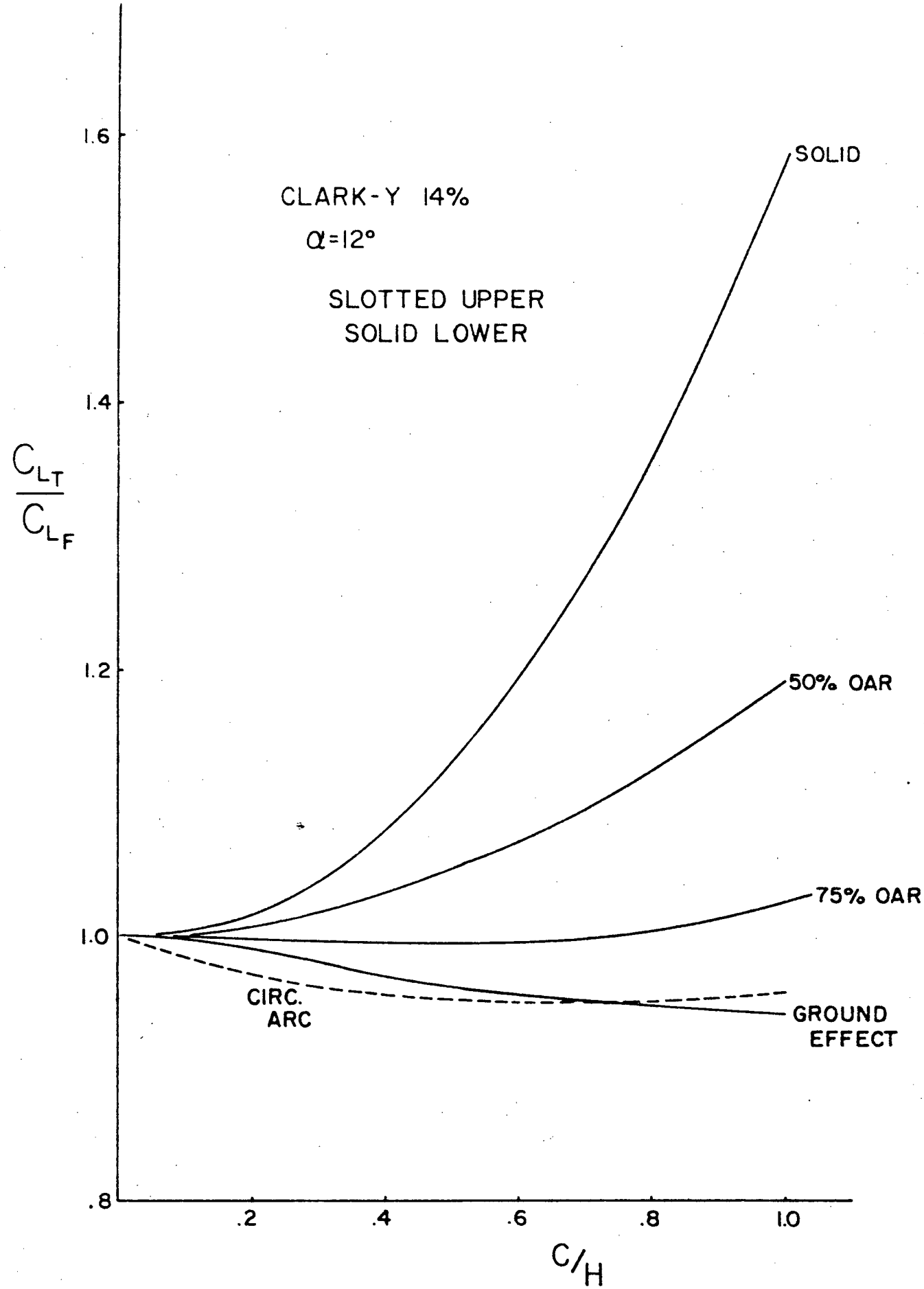

Figure 17. Variation of lift coefficient ratio with wall geometry for Clark-Y airfoil.

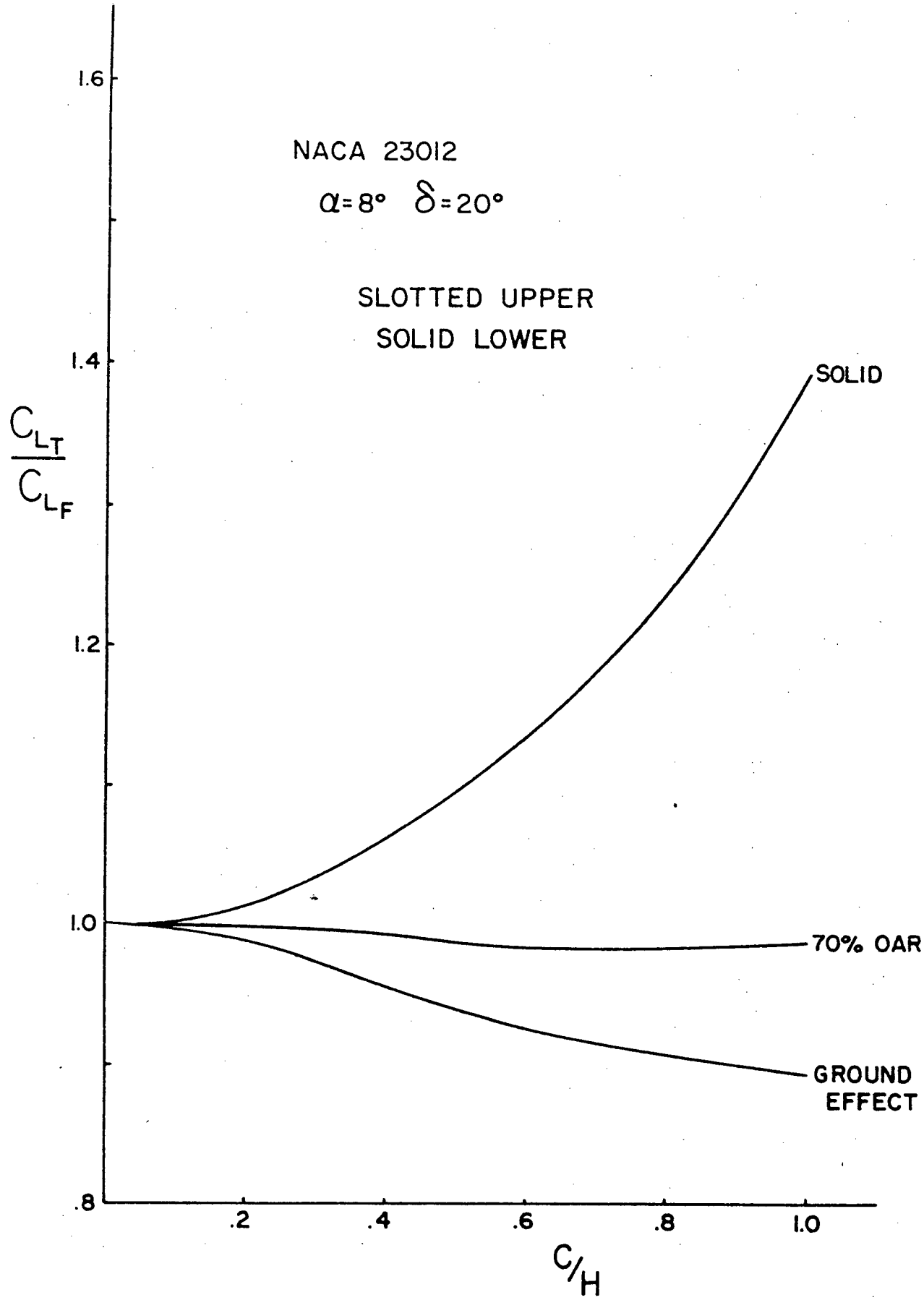

Figure 18. Variation of lift coefficient ratio with wall geometry for NACA 23012 airfoil with slotted flap.

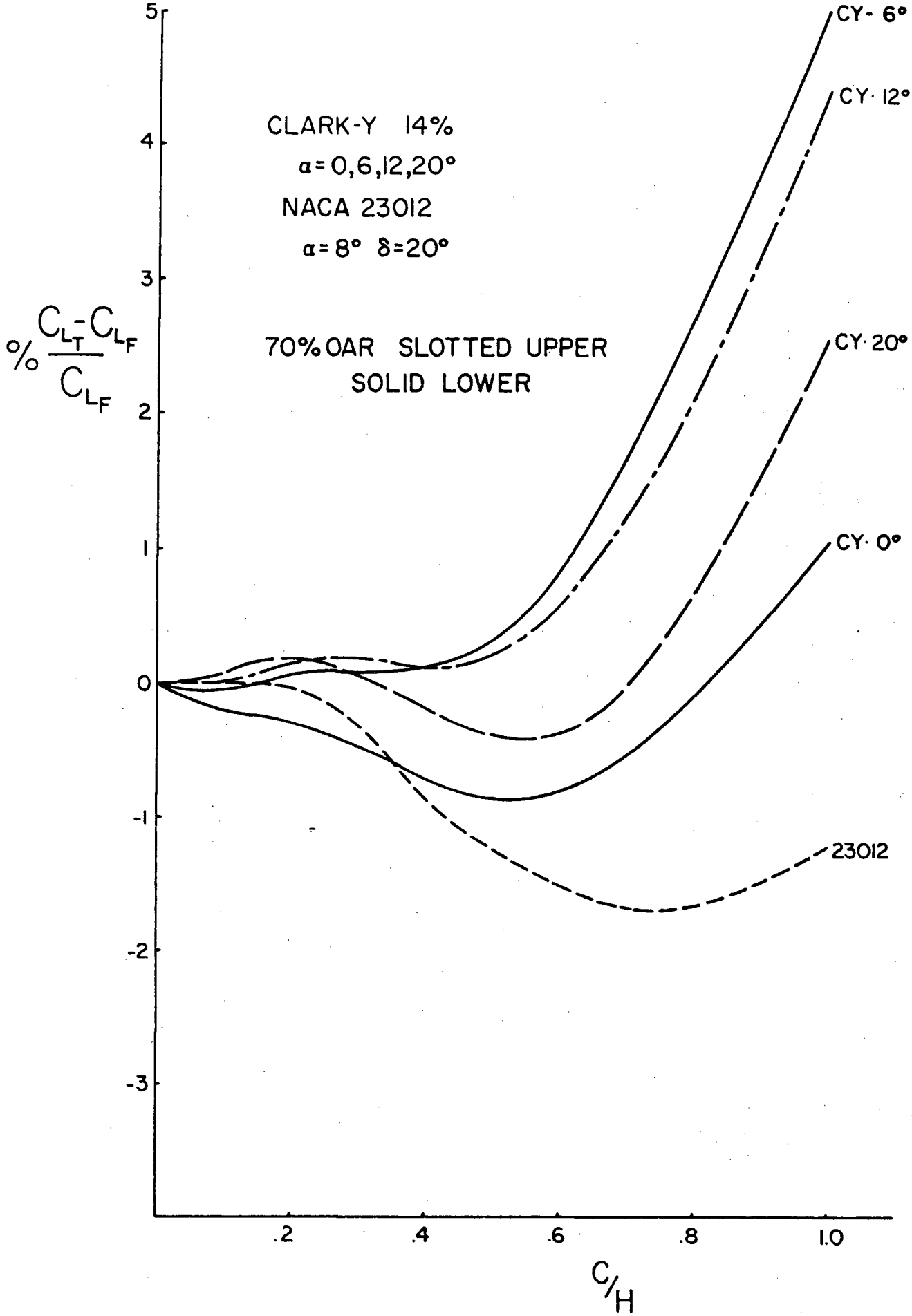

Figure 19. Relative error in lift coefficient for 70% upper wall open-area ratio.

Table 1. Configurations Tested

AF	α	NSA	WALL CONFIGURATION	NSU	NSL	NSLAT	c/C	t/c	NSS	OAR	NWC	C/H	CLF	CLT	CLT/CLF
C-Y	20	50	Solid	50	50	-	-	-	-	-	6.3	1.0	3.091	5.360	1.734
C-Y	20	50	Solid	50	50	-	-	-	-	-	6.3	.8	3.091	4.416	1.428
C-Y	20	50	Solid	50	50	-	-	-	-	-	6.3	.72	3.091	4.121	1.333
C-Y	20	50	Solid	50	50	-	-	-	-	-	6.3	.6	3.091	3.785	1.224
C-Y	20	50	Solid	50	50	-	-	-	-	-	6.3	.4	3.091	3.378	1.092
C-Y	20	50	Solid	50	50	-	-	-	-	-	6.3	.3	3.091	3.242	1.049
C-Y	20	50	Solid	50	50	-	-	-	-	-	6.3	.2	3.091	3.149	1.020
C-Y	20	50	Solid	50	50	-	-	-	-	-	6.3	.1	3.091	3.100	1.003
C-Y	12	50	Solid	100	100	-	-	-	-	-	6	1.0	2.188	3.475	1.585
C-Y	12	50	Solid	100	100	-	-	-	-	-	6	.8	2.188	2.982	1.360
C-Y	12	50	Solid	100	100	-	-	-	-	-	6	.6	2.188	2.622	1.195
C-Y	12	50	Solid	100	100	-	-	-	-	-	6	.4	2.188	2.372	1.080
C-Y	12	50	Solid	100	100	-	-	-	-	-	6	.2	2.188	2.225	1.015
C-Y	10	50	Solid	50	50	-	-	-	-	-	6.3	1.0	1.955	3.065	1.567
C-Y	10	50	Solid	50	50	-	-	-	-	-	6.3	.8	1.955	2.648	1.355
C-Y	10	50	Solid	50	50	-	-	-	-	-	6.3	.6	1.955	2.337	1.195
C-Y	10	50	Solid	50	50	-	-	-	-	-	6.3	.4	1.955	2.119	1.083
C-Y	10	50	Solid	50	50	-	-	-	-	-	6.3	.2	1.955	1.990	1.018
C-Y	0	50	Solid	50	50	-	-	-	-	-	6.3	1.0	.7635	1.115	1.460
C-Y	0	50	Solid	50	50	-	-	-	-	-	6.3	.8	.7635	.988	1.293
C-Y	0	50	Solid	50	50	-	-	-	-	-	6.3	.6	.7635	.889	1.163
C-Y	0	50	Solid	50	50	-	-	-	-	-	6.3	.4	.7635	.818	1.071
C-Y	0	50	Solid	50	50	-	-	-	-	-	6.3	.2	.7635	.775	1.013

AF	α	NSA	WALL CONFIGURATION	NSU	NSL	NSLAT	c/C	t/c	NSS	OAR	NWC	C/H	CLF	CLT	CLT/CLF
C-Y	-6.2	50	Solid	50	50	-	-	-	-	-	6.3	1.0	.0415	-.020	-1.39
C-Y	-6.2	50	Solid	50	50	-	-	-	-	-	6.3	.8	.0415	-.013	-.903
C-Y	-6.2	50	Solid	50	50	-	-	-	-	-	6.3	.6	.0415	-.004	-.290
C-Y	-6.2	50	Solid	50	50	-	-	-	-	-	6.3	.4	.0415	.0049	.338
C-Y	-6.2	50	Solid	50	50	-	-	-	-	-	6.3	.2	.0415	.0116	.80
C-Y	20	50	T.S.U.S.L.	-	80	15	.12	.33	9	.5	3.4	1.0	3.091	3.768	1.219
C-Y	20	50	T.S.U.S.L.	-	80	15	.12	.33	9	.5	3.4	.8	3.091	3.524	1.140
C-Y	20	50	T.S.U.S.L.	-	80	15	.12	.33	9	.5	3.4	.72	3.091	3.465	1.121
C-Y	20	50	T.S.U.S.L.	-	80	15	.12	.33	9	.5	3.4	.6	3.091	3.348	1.083
C-Y	20	50	T.S.U.S.L.	-	80	15	.12	.33	9	.5	3.4	.4	3.091	3.218	1.041
C-Y	20	50	T.S.U.S.L.	-	80	15	.12	.33	9	.5	3.4	.2	3.091	3.131	1.013
C-Y	20	50	T.S.U.S.L.	-	80	15	.06	.33	9	.75	3.4	1.0	3.091	3.062	.991
C-Y	20	50	T.S.U.S.L.	-	80	15	.06	.33	9	.75	3.4	.8	3.091	3.037	.983
C-Y	20	50	T.S.U.S.L.	-	80	15	.06	.33	9	.75	3.4	.72	3.091	3.033	.981
C-Y	20	50	T.S.U.S.L.	-	80	15	.06	.33	9	.75	3.4	.6	3.091	3.035	.982
C-Y	20	50	T.S.U.S.L.	-	80	15	.06	.33	9	.75	3.4	.4	3.091	3.063	.991
C-Y	20	50	G.E.	-	100	-	-	-	-	-	6	1.0	3.091	2.676	.866
C-Y	20	50	G.E.	-	100	-	-	-	-	-	6	.8	3.091	2.733	.884
C-Y	20	50	G.E.	-	100	-	-	-	-	-	6	.72	3.091	2.762	.894
C-Y	20	50	G.E.	-	100	-	-	-	-	-	6	.6	3.091	2.811	.909
C-Y	20	50	G.E.	-	100	-	-	-	-	-	6	.4	3.091	2.919	.944
C-Y	20	50	G.E.	-	100	-	-	-	-	-	6	.3	3.091	2.983	.965
C-Y	20	50	G.E.	-	100	-	-	-	-	-	6	.2	3.091	3.045	.985
C-Y	20	50	G.E.	-	100	-	-	-	-	-	6	.1	3.091	3.085	.998
C-Y	20	50	T.S.U.S.L.	-	80	15	.072	.33	9	.7	3.4	1.0	3.091	3.170	1.026
C-Y	20	50	T.S.U.S.L.	-	80	15	.072	.33	9	.7	3.4	.72	3.091	3.092	1.0
C-Y	20	50	T.S.U.S.L.	-	80	15	.072	.33	9	.7	3.4	.55	3.091	3.078	.996
C-Y	20	50	T.S.U.S.L.	-	80	15	.072	.33	9	.7	3.4	.39	3.091	3.087	.999
C-Y	20	50	T.S.U.S.L.	-	80	15	.072	.33	9	.7	3.4	.19	3.091	3.098	1.002

AF	α	NSA	WALL CONFIGURATION	NSU	NSL	NSLAT	c/C	t/c	NSS	OAR	NWC	C/H	CLF	CLT	CLT/CLF
C-Y	12	50	T.S.U.S.L.	-	80	15	.12	.33	9	.5	3.4	1.0	2.188	2.617	1.195
C-Y	12	50	T.S.U.S.L.	-	80	15	.12	.33	9	.5	3.4	.9	2.188	2.537	1.158
C-Y	12	50	T.S.U.S.L.	-	80	15	.12	.33	9	.5	3.4	.8	2.188	2.463	1.124
C-Y	12	50	T.S.U.S.L.	-	80	15	.12	.33	9	.5	3.4	.6	2.188	2.343	1.070
C-Y	12	50	T.S.U.S.L.	-	80	15	.12	.33	9	.5	3.4	.45	2.188	2.276	1.040
C-Y	12	50	T.S.U.S.L.	-	80	15	.12	.33	9	.5	3.4	.26	2.188	2.221	1.013
C-Y	12	50	T.S.U.S.L.	-	80	15	.12	.33	9	.5	3.4	.16	2.188	2.199	1.003
C-Y	12	50	T.S.U.S.L.	-	80	15	.06	.33	9	.75	3.4	1.0	2.188	2.234	1.021
C-Y	12	50	T.S.U.S.L.	-	80	15	.06	.33	9	.75	3.4	.6	2.188	2.179	.996
C-Y	12	50	T.S.U.S.L.	-	80	15	.06	.33	9	.75	3.4	.45	2.188	2.178	.994
C-Y	12	50	T.S.U.S.L.	-	80	15	.06	.33	9	.75	3.4	.26	2.188	2.187	.998
C-Y	12	50	T.S.U.S.L.	-	80	15	.06	.33	9	.75	3.4	.16	2.188	2.189	1.001
C-Y	12	50	T.S.U.S.L.	-	80	15	.06	.33	9	.75	3.4	.09	2.188	2.188	1.000
C-Y	12	50	T.S.U.S.L.	-	80	15	.072	.33	9	.7	3.4	1.0	2.188	2.284	1.044
C-Y	12	50	T.S.U.S.L.	-	80	15	.072	.33	9	.7	3.4	.8	2.188	2.233	1.021
C-Y	12	50	T.S.U.S.L.	-	80	15	.072	.33	9	.7	3.4	.6	2.188	2.200	1.006
C-Y	12	50	T.S.U.S.L.	-	80	15	.072	.33	9	.7	3.4	.45	2.188	2.190	1.001
C-Y	12	50	T.S.U.S.L.	-	80	15	.072	.33	9	.7	3.4	.26	2.188	2.192	1.002
C-Y	12	50	T.S.U.S.L.	-	80	15	.072	.33	9	.7	3.4	.16	2.188	2.190	1.001
C-Y	12	50	T.S.U.S.L.	-	80	15	.072	.33	9	.7	3.4	.09	2.188	2.188	1.000
C-Y	12	50	G.E.	-	100	-	-	-	-	-	6	1.0	2.188	2.060	.940
C-Y	12	50	G.E.	-	100	-	-	-	-	-	6	.8	2.188	2.068	.945
C-Y	12	50	G.E.	-	100	-	-	-	-	-	6	.6	2.188	2.087	.954
C-Y	12	50	G.E.	-	100	-	-	-	-	-	6	.4	2.188	2.121	.968
C-Y	12	50	G.E.	-	100	-	-	-	-	-	6	.2	2.188	2.170	.990

AF	α	NSA	WALL CONFIGURATION	NSU	NSL	NSLAT	c/C	t/c	NSS	OAR	NWC	C/H	CLF	CLT	CLT/CLF
C-Y	6	50	T.S.U.S.L.	-	80	15	.072	.33	9	.7	3.4	1.0	1.483	1.557	1.050
C-Y	6	50	T.S.U.S.L.	-	80	15	.072	.33	9	.7	3.4	.6	1.483	1.495	1.008
C-Y	6	50	T.S.U.S.L.	-	80	15	.072	.33	9	.7	3.4	.45	1.483	1.485	1.002
C-Y	6	50	T.S.U.S.L.	-	80	15	.072	.33	9	.7	3.4	.26	1.483	1.484	1.001
C-Y	6	50	T.S.U.S.L.	-	80	15	.072	.33	9	.7	3.4	.16	1.483	1.483	1.000
C-Y	6	50	T.S.U.S.L.	-	80	15	.072	.33	9	.7	3.4	.09	1.483	1.482	1.000
C-Y	0	50	T.S.U.S.L.	-	80	15	.072	.33	9	.7	3.4	1.0	.7635	.772	1.001
C-Y	0	50	T.S.U.S.L.	-	80	15	.072	.33	9	.7	3.4	.6	.7635	.758	.992
C-Y	0	50	T.S.U.S.L.	-	80	15	.072	.33	9	.7	3.4	.45	.7635	.757	.992
C-Y	0	50	T.S.U.S.L.	-	80	15	.072	.33	9	.7	3.4	.26	.7635	.761	.996
C-Y	0	50	T.S.U.S.L.	-	80	15	.072	.33	9	.7	3.4	.16	.7635	.762	.998
C-Y	0	50	T.S.U.S.L.	-	80	15	.072	.33	9	.7	3.4	.09	.7635	.762	.998
23012	8-20	81=46+35	Solid	100	100	-	-	-	-	-	6	1.0	2.442	3.300	1.392
23012	8-20	81	Solid	100	100	-	-	-	-	-	6	.8	2.442	3.009	1.233
23012	8-20	81	Solid	100	100	-	-	-	-	-	6	.6	2.442	2.770	1.135
23012	8-20	81	Solid	100	100	-	-	-	-	-	6	.4	2.442	2.587	1.061
23012	8-20	81	Solid	100	100	-	-	-	-	-	6	.2	2.442	2.472	1.012
23012	8-20	81	G.E.	-	100	-	-	-	-	-	6	1.0	2.442	2.176	.892
23012	8-20	81	G.E.	-	100	-	-	-	-	-	6	.8	2.442	2.212	.905
23012	8-20	81	G.E.	-	100	-	-	-	-	-	6	.6	2.442	2.261	.926
23012	8-20	81	G.E.	-	100	-	-	-	-	-	6	.4	2.442	2.330	.955
23012	8-20	81	G.E.	-	100	-	-	-	-	-	6	.2	2.442	2.413	.988

AF	α	NSA	WALL CONFIGURATION	NSU	NSL	NSLAT	c/C	t/c	NSS	OAR	NWC	C/H	CLF	CLT	CLT/CLF
23012	8-20	81	T.S.U.S.L.	-	80	15	.072	.33	9	.7	3.4	1.0	2.442	2.413	.988
23012	8-20	81	T.S.U.S.L.	-	80	15	.072	.33	9	.7	3.4	.8	2.442	2.402	.984
23012	8-20	81	T.S.U.S.L.	-	80	15	.072	.33	9	.7	3.4	.45	2.442	2.416	.989
23012	8-20	81	T.S.U.S.L.	-	80	15	.072	.33	9	.7	3.4	.26	2.442	2.439	.999
23012	8-20	81	T.S.U.S.L.	-	80	15	.072	.33	9	.7	3.4	.19	2.442	2.443	1.000
23012	8-20	81	T.S.U.S.L.	-	80	15	.072	.33	9	.7	3.4	.09	2.442	2.442	1.000

AF - Airfoil configuration.

α - Angle of attack-degrees.

NSA - Number of source and vortex elements on airfoil.

T.S.U.S.L. - Transversely slotted upper and solid lower walls.

G.E. - Airfoil in ground effect.

NSU - Number of source elements on upper solid wall.

NSL - Number of source elements on lower solid wall.

NSLAT - Number of airfoil-shaped slats.

c/C - Slat chord : airfoil chord ratio.

t/c - Slat thickness : chord ratio.

NSS - Number of source and vortex elements per slat.

NWC - Total extent of wall in airfoil chords.

REFERENCES

1. Allen,H.J. Vincenti,W.G. "Wall Interference in a Two-Dimensional Flow Wind Tunnel, with Consideration of the Effect of Compressibility". NACA TR 782, 1944

2. Baldwin,B.S. Turner,J.B. Knechtel,E.D. "Wall Interference in Wind Tunnels with Slotted and Porous Boundaries at Subsonic Speeds". NACA TN 3176, 1954.

3. Glauert,H. "Wind Tunnel Interference on Wings, Bodies and Airscrews". R&M 1566, British ARC 1933

4. Goldstein,S. "Two-Dimensional Wind-Tunnel Interference, Part II." R&M 1902, British ARC 1942.

5. Kellogg,O.D. "Foundations of Potential Theory". Dover

6. Lim,A.K. "Effects of Porous Tunnel Walls on High Lift Airfoil Testing". Thesis, UBC 1970.

7. Parkinson,G.V. "On the Use of Slotted Walls in Two-
Lim,A.K. Dimensional Testing of Low-Speed Airfoils".
CASI Trans. 4, Sept. 1971.

8. Smith,A.M.O. "Calculation of Potential Flow about
Hess,J.L. Arbitrary Bodies".
Progress in Aeronautical Sciences Vol.8,
1967.

9. Tomotika,S. "The Lift and Moment on a Circular-Arc
Tamada,K. Airfoil in a Stream Bounded by a Plane
Wall".
Umemoto,H. QJMAM Vol.4, 1950.

10. Wenzinger,C.J. "Pressure Distribution over an NACA 23012
Delano,J.B. Airfoil with a Slotted and a Plain Flap".
NACA TR633, 1938.

11. Wood,W.W. "Tunnel Interference from Slotted Walls".
QJMAM Vol.17, Part 2, 1964.

12. Woods,L.C. "The Theory of Subsonic Plane Flow".
Cambridge, 1961.